MONOCLONAL ANTIBODIES SPECIFIC FOR THE PUTATIVE CANCER SIGNALING PROTEIN, UEV1A

A Thesis Submitted to the College of

Graduate Studies and Research

In Partial Fulfillment of the Requirements

For the Degree of Masters of Science

In the Department of Microbiology and Immunology

University of Saskatchewan

Saskatoon

By

LINDSAY PELZER

PERMISSION TO USE

In presenting this thesis in partial fulfilment of the requirements for a Postgraduate degree from the University of Saskatchewan, I agree that the Libraries of this University may make it freely available for inspection. I further agree that permission for copying of this thesis in any manner, in whole or in part, for scholarly purposes may be granted by the professor or professors who supervised my thesis work or, in their absence, by the Head of the Department or the Dean of the College in which my thesis work was done. It is understood that any copying or publication or use of this thesis or parts thereof for financial gain shall not be allowed without my written permission. It is also understood that due recognition shall be given to me and to the University of Saskatchewan in any scholarly use which may be made of any material in my thesis. Requests for permission to copy or to make other use of material in this thesis in whole or part should be addressed to:

Head of the Department of Microbiology and Immunology

University of Saskatchewan

Saskatoon, SK, S7N 5E5

ABSTRACT

UEV1A and *MMS2* are two human genes whose proteins share greater than ninety percent sequence identity. Both Uev1A and Mms2 are ubiquitin-conjugating enzyme variants (Uev) that lack the active cystine residue required for the ubiquitin conjugation reaction. They work with the ubiquitin-conjugating enzyme Ubc13 to create Lys63-linked polyubiquitin chains which have recently been found to cause cellular signals not involving target protein degradation. Only the Mms2-Ubc13 complex functions in DNA repair in mammalian cells. In contrast, only the Uev1A-Ubc13 complex is involved in TRAF2- and TRAF6-mediated NF-κB activation by ubiquitinating NEMO/IKKγ. *UEV1B* is a splice variant of *UEV1A* containing different N-terminal coding sequences and its cellular function is currently unknown.

The NF-κB signaling pathway has been regarded as a primary pro-survival and anti-apoptotic response. *UEV1A* expression is positively correlated to tumor formation, suggesting that it plays a role in tumorigenesis. Furthermore, experimental overexpression of *UEV1A* alone is sufficient to activate NF-κB, which is reversible upon suppression of *UEV1A* expression by RNA interference. Overexpression of *UEV1A* also protects cells from stress-induced apoptosis and confers a growth advantage under serum-deprived conditions. These observations collectively support *UEV1A* as a candidate proto-oncogene.

The objective of this research was to obtain monoclonal antibodies (Mabs) capable of recognizing Uev1, but not Mms2. This is a challenging task given very few possible epitopes that may distinguish the two proteins. The four sequences unique to Uev1A are located in the 30 a.a. N terminal region, the single substitution at a.a. 104, the 14 a.a. core region from a.a. 116-129 (7/14 variable) and the C-terminus at a.a. 167-169.

Hybridoma cells were produced vis á vis fusions of B cells from Uev1A-immunized mice with FO myeloma cells lacking the ability to produce immunoglobulin. The hybridoma cells were screened using enzyme immunoassays (EIAs) for reactivity with Uev1A and Mms2. Ascities fluid was produced for five Mabs named LN1, LN2, LN2A, LN2B and LN3. EIA and Western blotting of Uev1A-deletion constructs revealed that Mab LN1 binds specifically to amino acids (a.a.) 10-30 of the unique Uev1A N-terminal sequence, that Mabs LN2, LN2A and LN2B bind specifically to the unique a.a. 110-130 region of Uev1A, and that Mab LN3 binds specifically to a.a. 30-44 of Uev1A common to Mms2.

Competition analysis of unconjugated Mabs versus horse radish peroxidase (HRP)-conjugated Mabs for binding to Uev1A permitted epitope mapping for the five Mabs. The results indicate that Mabs LN1 and LN3 inhibit each other from binding to their distinct sequences which are spatially adjacent. Mabs LN2 and LN2B inhibit each other, but not Mab LN2A. Additionally, Mab LN2A is unable to inhibit Mabs LN2 or LN2B. In summary, Mabs have been aquired to three catergories which were originally desired: one to the unique N-terminus (Mab LN1), three to the unique core sequence (Mabs LN2, LN2B and LN2A), and one to the same region Ubc13 binds to Uev1A and Mms2 (Mab LN3). The potential applications of these Mabs are discussed.

ACKNOWLEDGEMENTS

I would like to thank those significant people who have assisted me in the successful completition of this Master's degree. Firstly, I thank Dr. Wei Xiao for providing me with an incredible thesis objective which I am very proud to have accomplished and, for his indisputably remarkable supervision. Secondly, I thank Dr. Barry Ziola for challenging me constantly. I believe he has constructively shaped my scientific mind and my character. I thank him profusely for taking me under his wing.

I would like to thank my committee members Dr. Xiao, Dr. Ziola and Dr. Geyer for their unvarying generosity with their time especially during the writing and defense process. I would also like to thank my external examiner Dr. Lou Qualtiere for his generosity with his time for the Master's defense.

A big thank you must go to the entire Dr. Wei Xiao laboratory, especially to exceptional members of the lab Dr. Landon Pastushok, and Parker Andersen. Both these men spent countless hours educating me with a myriad of skills and knowledge and I must thank them for their continuous support. I also thank Michelle Hanna and Lindsay Ball for providing me not only with enlightening scientific discussion but also with their friendship. Additionally, I also thank Monique Haakensen for providing me with many long days of entertainment and conversation in Dr. Ziola's lab.

I would like to extend an imperative thank you to the support staff in the department of microbiology and immunology, namely, Vern, Katie, Mary, Dawn and Sherry.

I thank my parents for always providing me with unconditional love, support and encouragement. The motivational force I experience to achieve has been ingrained as a part of me for as long as I can remember. I thank my parents for instilling such undying

motivation and for the conviction that I can achieve anything I put my mind to. I hope they are proud.

Lastly, I would like to thank my husband Rob Pelzer. Thank you for your never-ending honesty, encouragement, support, patience and love. You are an incredible husband and I thank you for having been especially supportive while I worked towards this degree.

TABLE OF CONTENTS

page

LIST OF TABLES

LIST OP FIGURES

LIST OF ABBREVIATIONS

A	Aminopterin
a.a.	amino acids
ADC	Antibody-Drug Conjugates
ATP	Adenosine 5'-Triphosphate
Bcl-2	B-cell leukemia/ lymphoma 2
bp	base pair
EDTA	Ethylenediaminetetraacetic acid
EIA	Enzyme Immunoassay
E-tube	Eppendorf-tube
Fab	Fragment antigen binding
Fc	Fragment crystallisable
GST	Gluthathione-S-Transferase
HAMA	Human Anti-Mouse Antibodies
HAT	Hyoxanthine Aminopterin Thymidine
HRP	Horseradish Peroxidase
IκB	Inhibitor of κB protein kinase
IKK	IκB kinase
IPTG	isopropyl-β-D-thiogalactopyranoside
LB	Luria broth
Mabs	Monoclonal Antibodies
MHC	Major Histocompatibility Complex
MW	Molecular Weight
NEMO	NF-κB Essential Modulator

NF-κB	Nuclear factor kappa B
ORF	Open Reading Frame
P	Phosphorylation
PBS	Phosphate Buffered Saline
PEG	Polyethylene Glycol
PCNA	Proliferating Cell Nuclear Antigen
PCR	Polymerase Chain Reaction
PVDF	Polyvinylidene Difluoride
rd	reverse osmosed
RIP	receptor interacting protein 1
RPMI	Roswell Park Memorial Institute
RT	Room Temperature
SDS-PAGE	Sodium Dodecyl Sulfate Polyacrylamide Gel Electrophoresis
SOC	Super Optimal Catabolite repression
TNFα	Tumor necrosis factor alpha
TNFR	Tumor necrosis factor receptor
TRADD	TNF receptor associated death domain
TRAF2	Tumor necrosis factor receptor-associated factor 2
TRAF6	Tumor necrosis factor receptor-associated factor 6
V(D)J	Variable Diversity Joining
Ub	Ubiquitin
Uba	Ubiquitin-activating enzyme
Ubc	Ubquitin-conjugating enzyme
Ubl	Ubiquitin ligase
Uev	Ubiquitin-conjugating enzyme variants

CHAPTER ONE

LYS63-LINKED UBIQUITINATION AND CANCER

Ubiquitin (Ub) is one of the most conserved proteins found in all eukaryotic organisms. It exists as a free cellular monomer or it can be covalently modified in monomers or chains onto target intracellular proteins (Hershko, 1998). The 76 amino acid (a.a.) Ub polypeptide is critical for many cellular processes such as stress responses, cell cycle progression, oncongenesis and antigen presentation (Hofmann and Pickart, 1999). Ubiquitination, the attachment of Ub to a target protein, requires the formation of an isopeptide bond between the C-terminal Gly76 on Ub and a Lys residue on the target protein via a series of steps (Hochstrasser, 1996).

In this ubiquintination process, Ub is first activated by an Ub-activating enzyme (Uba) in the presence of adenosine 5'-triphosphate (ATP), forming a high-energy Uba-Ub thiolester bond. The activated Ub is then transferred from Uba to a specific thiol of an Ub-conjugating enzyme (Ubc) to form an Ubc-Ub thiolester. The Ub of Ubc-Ub is further transferred to the target protein either alone or with a Ub ligase (Ubl). The Ub surface Lys residues serve as the substrates for other Ub proteins to bind and form Lys-linked Ub chains (Chau et al., 1989). Ub has seven surface Lys residues, creating the potential for seven distinct types of chains, at least five of which have been observed *in vitro* or *in vivo* (Volk et al., 2005). It has become clear that the signaling properties of Ub depend on the topology of the linakage in which the chains are constructed. Of the five Ub linkages observed *in vitro* or *in vivo*, only two linkages have been well studied. The well established Gly76-Lys48-linked polyubiquitin chains signal for target proteins to be

transported to the 26S proteasome for degradation (Hershko and Ciechanover, 1992; Hochstrasser, 1996; Hoege et al., 2002; Hofmann and Pickart, 1999). Alternatively, proteins can also be ubiquitinated through the non-canonical Gly76-Lys63-linkage, which in recent years has shown to regulate the function of diverse proteins in a nonproteolytic manner (Hofmann and Pickart, 1999). In fact, Gly76-Lys63-linked chains have been implicated in DNA damage tolerance, mitotic checkpoint pathways and Nuclear factor kappa B (NF-κB) activation (Andersen et al., 2005; Bothos et al., 2003; Broomfield et al., 1998).

1.1 Lys63-linked polyubiquitin chains and cellular signaling

To date, Ubc13 is the only known Ubc enzyme capable of catalyzing the Lys63-linked polyubiquitination reaction, which also requires a ubiquitin conjugating enzyme variant (Uev) as a co-factor (Hofmann and Pickart, 1999; McKenna et al., 2001). A Uev is defined as a protein that resembles Ubc in structure and a.a. sequence, but does not contain a Cys residue in the active site, rendering the protein catalytically inactive (Broomfield et al., 1998; Sancho et al., 1998). Ubc13 has a conserved Ubc family catalytic domain, which contains an active site Cys residue, allowing it to conjugate Ub (Hofmann and Pickart, 1999). Regulation of Ubc13 activity depends on which Uevs are assisting with the formation of the chain (Andersen et al., 2005). Neither Ubc13 nor Uev alone are able to promote polyubiquitin chains (Hofmann and Pickart, 1999).

Ubc13 creates Lys63-linked polyubiquitin chains with the Uevs Mms2 and Uev1A in the DNA damage tolerance and NF-κB signaling processes, respectively. Ubc13 physically interacts with Mms2 (Hofmann and Pickart, 1999) to promote error-free DNA damage tolerance (Broomfield et al., 1998) by polyubiquitination of the proliferating cell nuclear antigen (PCNA) via Lys63-linked chains (Hoege et al., 2002),

as has been shown in the model eukaryotic organism *Saccharomyces cerevisiae*. Alternatively, Ubc13 physically interacts with Uev1A to promote NF-κB activation (Deng et al., 2000) by polyubiquitination of NF-κB essential modulator (NEMO) via Lys63-linked chains (Andersen et al., 2005). The entire pathway is explained and discussed in Section 1.3.

1.2 Mms2 and Uev1A sequence, structure and functional similarities

Both Mms2 and Uev1A interact with Ubc13 for Lys63-linked polyubiquitination of target proteins. Additionally, Mms2 and Uev1A share 90% identity in sequence (Figure 1-1) and, although they both facilitate Lys63-linked polyubiquitin chain assembly, they function in distinct cellular processes as mentioned in section 1.1. Crystal structures have revealed that the Mms2 monomer undergoes a localized conformational change upon interaction with Ubc13 (Moraes et al., 2001). The structure of the human Mms2–Ubc13 complex provides the foundation for understanding the mechanism of Lys63 polyubiquitin chain assembly. A T-shaped heterodimer is formed that allows Mms2 to orient an acceptor Ub through non-covalent contacts such that its Lys63 residue is presented to the donor Ub at the Ubc13 active site. An isopeptide bond can then be formed between the two molecules and Lys63 di-Ub is free to exit through a channel leading from the Ubc13 active site toward a Ubl-binding site (McKenna et al., 2003; McKenna et al., 2001). Mms2 is necessary for this process and, based on Ubc13-Mms2 crystal structures, Mms2-Phe13 is responsible for the interaction between these two proteins (Pastushok et al., 2005). It is understood that the Uev1A-Ubc13 heterodimer possesses the same binding properties in order to assemble Lys63-linked polyubiquitin chains. Figure 1-2 depicts a Uev1A-Ubc13 T-shaped heterodimer, donor and acceptor ubiquitins for the assembly of Lys63-linked Ub chains. Within the 90% sequence identity

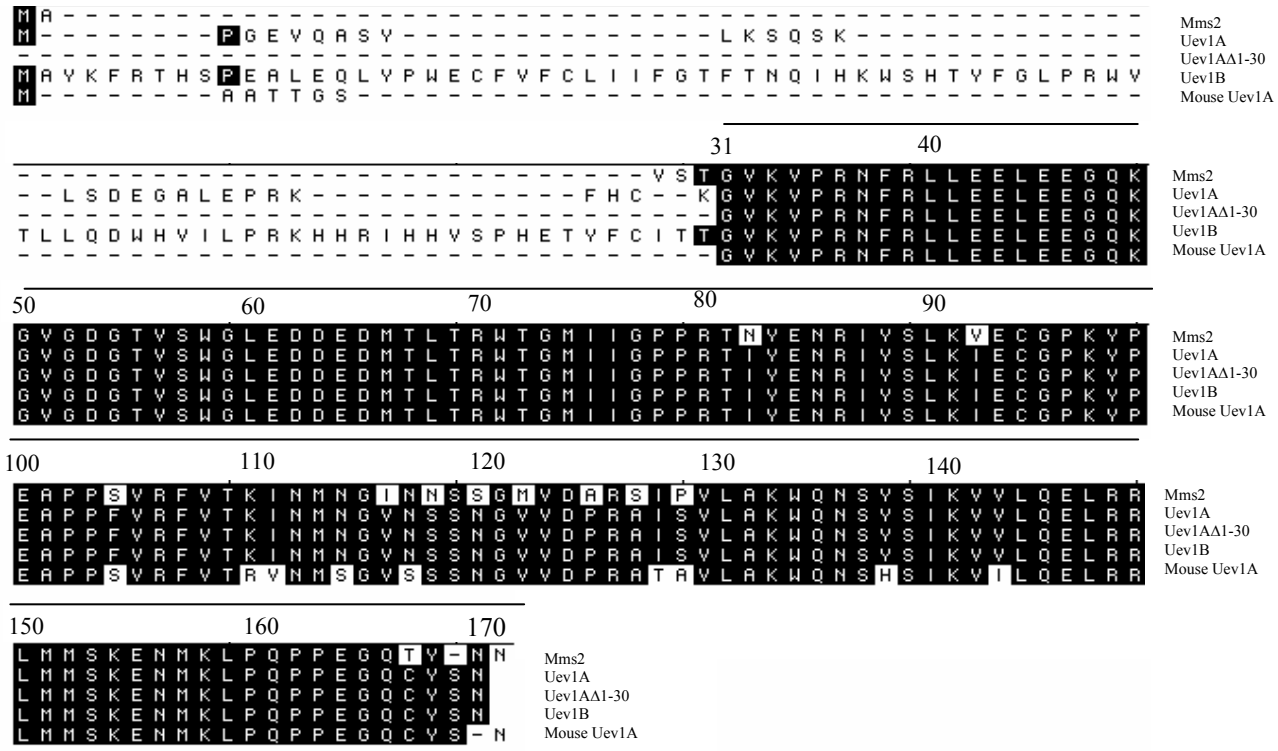

Figure 1-1. **Amino acid sequence comparison of human Ubc variants Mms2, Uev1A Uev1AΔ1-30, Uev1B and mouse Uev1A.** Numbering begins at a.a. 31 of human Uev1A to illustrate the differing sequences of human Mms2, human Uev1B and mouse Uev1A N-terminal to Gly 31. Mms2, Uev1A and Uev1B do not share sequence similarity in their N-terminal a.a. Uev1A and Uev1B share identical core sequences which differ from Mms2.

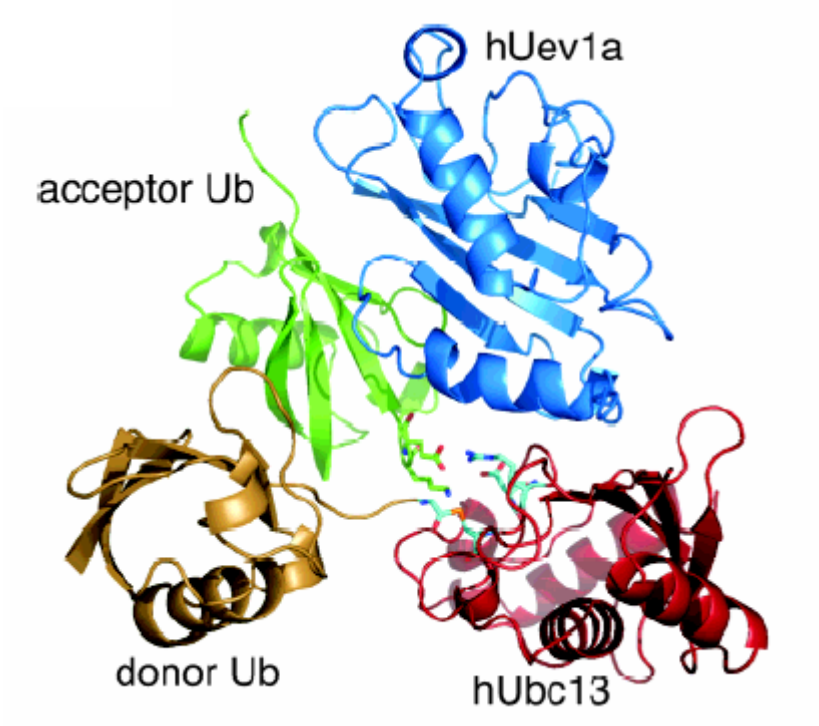

Figure 1-2. Molecular surface of Uev1A-Ubc13 heterodimer. Surface of the Uev1A-Ubc13 heterodimer. Uev1A is colored in blue, Ubc13 in red, acceptor Ub in green and donor Ub in gold (Hau et al., 2006).

of Uev1A and Mms2, they share the ubiquitin and Ubc13 binding sites. Thus, the binding sites of Ub and Ubc13 to Uev1A are identical to Mms2.

Given that both Uev1A and Mms2 are able to form a stable complex with Ubc13 in *vivo* and *in vitro*, but their biological functions are distinct, the structural and sequence differences between Uev1A and Mms2 are presumed to be responsible for their functionally distinct intracellular signaling pathways (Andersen et al., 2005). However, it is not known whether the N-terminal 30 a.a., the one a.a. substitution at 104, the seven unique a.a. in the core region or the C-terminal two a.a. are responsible for the important functional differences between Uev1A and Mms2. Interestingly, Uev1A has been implicated in tumorigenesis due to its role in NF-κB activation, whereas Mms2 has no role in this process (Andersen et al., 2005).

1.3 Ubc13-Mms2 heterodimer function in error-free postreplication repair

The living cell is susceptible to spontaneous and environmental DNA damage. Genome instability may cause cell death, carcinogenesis, mutational genetic variability and ageing when such damage is incurred. Eukaryotic DNA repair pathways are highly conserved from yeast to humans. Three epistasis groups have been identified with respect to eukaryotic DNA repair mutants (Prakash et al., 1993). The RAD3 group mediates nucleotide excision repair, the RAD52 group mediates double-strand break repair and the RAD6 group acts on the stalled replication machinery that has encountered a damaged template (Prakash et al., 1993). The RAD6 mode of repair seems to be employed through at least two different RAD6-dependent mechanisms (Xiao et al., 1999). Firstly, error-prone DNA repair uses particular translesion polymerases that place correct or incorrect nucleotides across a damaged site. Secondly, the other RAD6-dependent mode is error-free because it inserts the correct nucleotide by using the information found

on the undamaged sister duplex at the replication fork. Yeast Mms2 is required for this error-free mode of post replication repair to prevent spontaneous and damage-induced mutagenesis and genome instability (Broomfield et al., 1998). The yeast Ubc13–Mms2 complex targets PCNA for Lys63 Ub chain assembly (Hoege et al., 2002). However, proteins important for DNA repair that are targeted by Mms2-Ubc13 have remained unidentified. The Mms2-Ubc13 complex is therefore regarded as a defender against genome instability and carcinogenesis, whereas the Uev1A-Ubc13 complex is regarded as an activator of an anti-apoptotic and carcinogenic pathway.

1.4 Ubc13-Uev1A heterodimer function in NF-κB activation

There are five proteins which belong to the NF-κB family (Gilmore, 2006). These are called NF-κB1 (p50/p105), NF-κB2 (p52/p100), RelA, RelB and c-Rel. All proteins of the NF-κB family share a Rel homology domain in their N-terminal halves. NF-κB1 and NF-κB2 proteins are synthesized as large precursors, p105 and p100, which undergo processing to generate the mature NF-κB subunits, p50 and p52, respectively. The processing of p105 and p100 is mediated by the Ub/proteasome pathway and involves selective degradation of their C-terminal region. While the generation of p52 from p100 is a tightly regulated process, p50 is produced from constitutive processing of p105 (Karin and Ben-Neriah, 2000; Senftleben et al., 2001). From this point in this thesis, when NF-κB is written it will refer to p50 and p65.

Activation of the NF-κB signal transduction pathway is normally initiated by extracellular signals such as tumor necrosis factor α (TNFα), interleukins, ultraviolet irradiation and bacterial or viral infections. As is illustrated in Figure 1-3, receptor activation signals a cascade of events that eventually unite onto inhibitor of κB kinase (IKK). IKK consists of two kinase subunits (IKKα and IKKβ) and a regulatory subunit [IKKγ or NF- kB Essential Modulator (NEMO)]. Essentially, this frees the NF-κB

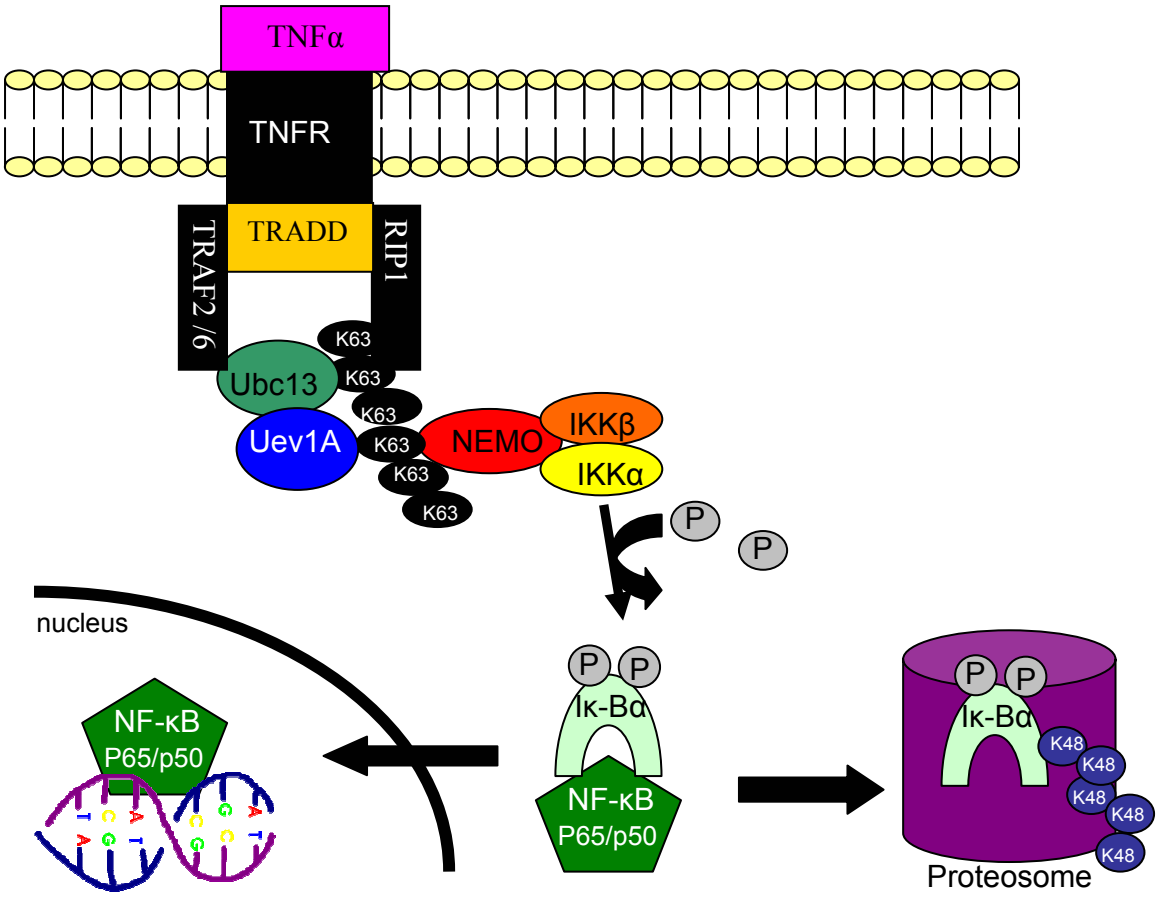

Figure 1-3. NF-κB activation following ubiquitination of NEMO/IKKγ by Uev1A-Ubc13. TNFα binding to its receptor, tumor necrosis factor receptor (TNFR), initiates the interaction between tumor necrosis factor receptor associated death domain (TRADD), receptor interacting protein 1(RIP1) and tumor necrosis factor associated-factor 2/6 (TRAF2/6). Ubc13 and Uev1A act as an Ub-conjugating enzyme heterodimer to ubiquintate NEMO and RIP1 through Lys63-linked Ub chains. This is required for IκBα phosphorylation and, subsequently, NF-κB activation. NF-κB can then freely travel into the nucleus where it acts as a transcription factor for activating cell survival genes. Figure adapted from Syed et al., 2006.

transcriptional activator to translocate into the nucleus and activate an array of target genes (Hayden and Ghosh, 2004), while IκBα is targeted to the 26S proteosome through Lys48-linked polyubiquitination.

The role of Lys63 polyubiquitin modifications in the NF-κB cascade has recently received considerable attention. NEMO/IKKγ is a cellular target of Lys63 polyubiquitination, which requires the Ubc13-Uev1 complex with TRAF2 or TRAF6 as a Ubl (Deng et al., 2000). The Ubc13-Uev1 heterodimer is also involved in Lys63 polyubiquitination of RIP1 (Wertz et al., 2004), which is required for NF-κB activation in response to TNFα (Lamothe et al., 2007). Ubc13-Uev1A dependent Lys63-linked polyubiquitination of NEMO/IKKγ activates IKK to phosphorylate IκBα, an inhibitory protein that retains NF-κB subunits in the cytoplasm. NF-κB is a transcription factor that regulates immune responses and inflammation through the expression of many genes, including those coding for cytokines, chemokines and adhesion molecules (Perkins, 2006). Once NF-κB has been freed to translocate to the nucleus, following phosphorylation of Iκ-Bα, it acts as a transcription factor for over 150 genes. These genes are in categories of chemokines/cytokines, immunoreceptors, antigen presentation, cell adhesion molecules, acute phase proteins, stress response genes, cell surface receptors, regulators of apoptosis, growth factors/ ligands, early response genes and transcription factors/ regulators. NF-κB can be considered a proto-oncogene as its activation has been implicated in many cancers and other diseases

1.5 NF-κB or Uev1A overexpression causes uncontrollable cellular proliferation

Analysis of NF-κB-deficient mice and cells led to the discovery of a novel function for this versatile transcription factor in the inhibition of apoptosis as seen in Figure 1-4. One study found that mice deficient in NF-κB died at embryonic day 15 due

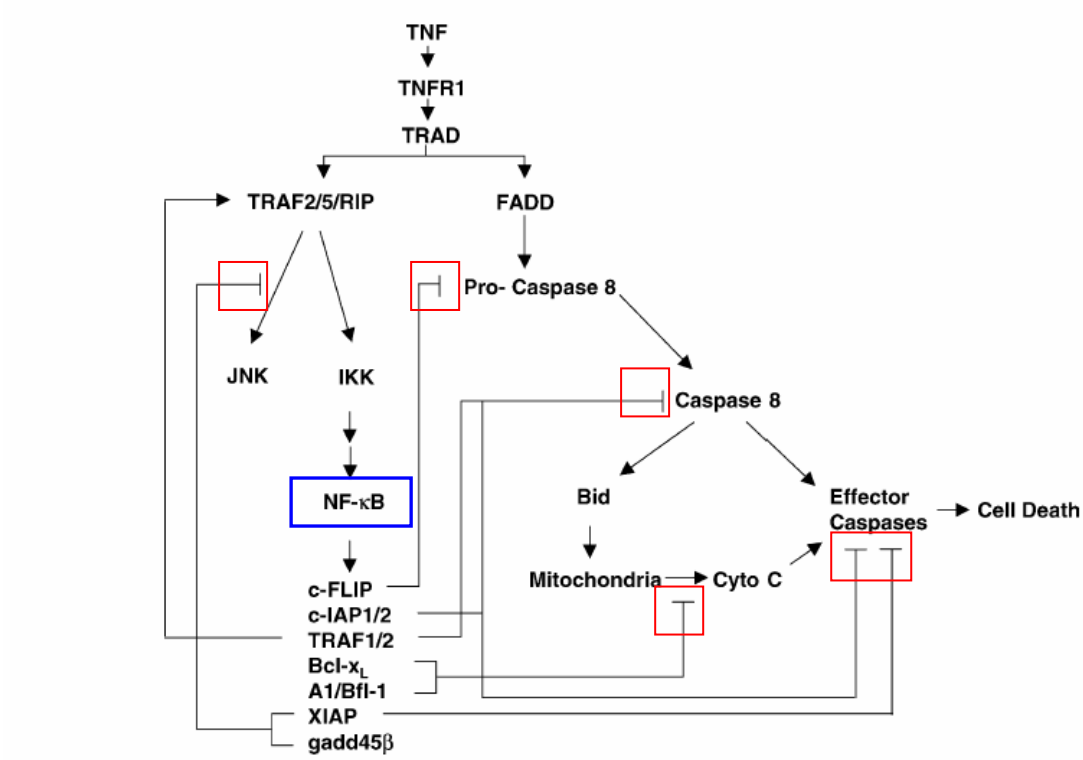

Figure 1-4. NF-κB is a transcription factor responsible for regulating anti-apoptosis. Downstream genes transcriptionally activated by NF-κB directly inhibit caspase and the mitochondrial cytochrome C apoptotic pathways (Lin and Karin, 2003).

to massive apoptosis of the hepatocytes in the liver (Beg et al., 1995). NF-κB-deficient mouse fibroblasts were also found to exhibit enhanced sensitivity to pro-apoptotic stimuli such as TNFα. TNFα is a poor inducer of apoptosis unless RNA or protein levels are low. However, when there was a deficiency in NF-κB and these cells were primed with TNFα, apoptosis was evident. Activation of NF-κB ablates TNFα's pro-apoptotic activity (Beg and Baltimore, 1996; Van Antwerp et al., 1996). This is because certain NF-κB target genes code for inhibitors of caspase activation and apoptosis (Kucharczak et al., 2003). The suppression of apoptosis by NF-κB is an important component of TNFα biology. In addition to suppression of TNFα-induced apoptosis, NF-κB inhibits apoptosis induced by a variety of DNA-damaging chemotherapeutic drugs and ionizing radiation in epithelial cells (Papa et al., 2004; Sakon et al., 2003).

Cellular mutational events leading to overexpression of NF-κB amplifies anti-apoptotic signaling. Recent discoveries show that Uev1A overexpression may also play a role in tumorigenesis. Uev1A has been recognized to be upregulated in immortal cells. Specifically, a five- to six-fold elevation in *UEV1A* expression was observed in SV40-transformed human embryonic kidney cells immediately following proliferative crisis, suggesting a potential role for these genes in immortalization (Ma et al., 1998). *UEV1A* expression has been shown to be increased in a variety of immortal tumor-derived cell lines compared to their normal tissue (Broomfield et al., 1998; Ma et al., 1998). Simply stated, Uev1A activates NF-κB, which assists in anti-apoptosis signaling. If any of the Activating proteins in this signaling pathway were mutationally overexpressed, oncogenesis could result. Constitutive high-level expression of *UEV1A* alone in cultured human cells was found to be sufficient to cause a significant increase in NF-*κ*B activity as well as the expression of its target anti-apoptotic protein, Bcl-2 (B-cell leukemia/ lymphoma 2) (Syed et al., 2006). Overexpression of *UEV1A* also allowed prolonged cell

survival under serum-deprived conditions and protected cells against apoptosis induced by diverse stressing agents. All effects seen with overexpression of *UEV1A* were reversible upon suppression of expression by RNA interference (Syed et al., 2006). Hence, Uev1A is a critical regulatory component in the NF-κB signaling pathway and is a potential proto-oncogene. As some tumor cells have been shown to exhibit constitutive Uev1A activity (Broomfield et al., 1998), targeting Uev1A may be critical for successful cancer therapy.

1.6 Rationale for targeting Uev1A: the unique challenge of this research project

Many observations, thus, collectively support *UEV1* as a candidate proto-oncogene. Therefore, obtaining a reagent capable of recognizing (and hopefully neutralizing Uev1A?), but not Mms2 is of significant interest. This is a challenging task given that only a few epitopes are expected to exist that could be employed to distinguish the two proteins. Uev1A and Mms2 differ at a.a. 82 and 92, however, these a.a. are not expected to be important for function as they are located within the interior of the folded protein structure. The four unique sequences of Uev1A to be targeted are located in the 30 a.a. N-terminal sequence, a.a. 104, the 14 a.a. core region around a.a. 116-129 (7/14 variable) and the four a.a. C-terminal sequence (2/4 variable) as can be observed in the a.a. sequence alignment in Figure 1-1. Recognition of these unique Uev1A sequences could conceivably target Uev1A, but not Mms2 *in vitro* and *in vivo.* This could ultimately allow additional experimental characterization of the functional differences between Mms2 and Uev1A as well as facilitate recognition of Uev1A in human tumor tissues.

CHAPTER TWO

HYBRIDOMA TECHNOLOGY

2.1 The immune response to a foreign antigen

The immune system harbors many lines of defense against invading foreign antigens. The first line of defense against invaders consists of physical barriers such as skin and mucosal membranes of the digestive, respiratory and reproductive tracts. The innate immune system acts as the first line of defense once an invader has broken through the physical barriers of the organism. The innate immune system includes neutrophils, macrophages, natural killer cells and the complement system that act together to respond quickly and strongly to invasion. Vertebrates have a third level of defense, of most importance to this particular research, which is the adaptive immune system.

2.2 B cell function in the immune response

The adaptive immune system uses a complex system of signaling between the B cell lymphocyte, the T cell lymphocyte and either an array of specialized cells or the complement system to dispose of foreign antigens. B cells have antibodies on their surfaces which specifically bind to a foreign antigen (Ambrus and Fauci, 1985; Ollila and Vihinen, 2005). This antigen-antibody complex is taken up by the B cell and chewed up by proteolysis into smaller peptides (Krieger et al., 1985). The B cell displays these antigenic peptides on its surface major histocompatibility complex (MHC) class II molecules. This combination of MHC and antigen attracts a matching helper T cell, which releases lymphokines and activates the B cell (Reinherz et al., 1980). The activated

B cell then begins to divide and progeny cells secrete millions of copies of the antibody. These antigen-specific antibodies circulate in blood plasma and lymph and bind to any additional identical antigens present (Ollila and Vihinen, 2005). Subsequently, this opsonizes the antigen for destruction by complement activation or for uptake and destruction by neutrophils, macrophages and natural killer cells.

2.3 Antibody structure, classes and isotypes in mice

Antibodies are usually shown as Y shaped structures with four subunits. As is shown in Figure 2-1, antibody molecules have two longer subunits called heavy chains and two shorter subunits called light chains (Capra et al., 1975). Two types of light chains exsist, κ and λ, of which only one kind will exist in any one antibody molecule (Riesen, 1980). The heavy chains are linked to each other and to the light chains by disulfide bridges. Two important antibody regions were originally determined upon digestion with the enzyme papain (Porter, 1959). The antigen-recognition region of the antibody is called Fab for 'fragment antigen binding'. This region contains the N-terminal sequences of both the heavy and light chains. The C-terminal sequence of the antibody molecule is called the Fc portion for 'fragment crystallisable' as it was orginally found to be crystallised at 4ºC. The Fc portion of the antibody molecule can be imbeded into the cellular surface of the B cell to target antigen binding thereby causing cell proliferation and excretion of identical antibody molecules from these cells (Natvig and Kunkel, 1973). Recombination of the constant region confers whether the antibody will be secreted or membrane bound. IgM and IgD antibodies can be found imbedded in the B cell membrane. Additionally, the Fc portion of secreted antibodies is recognized by other immune system cells in order to remove the antigen-antibody complex from the individual's body. Five classes of antibodies exist which are named IgG, IgA, IgM, IgD,

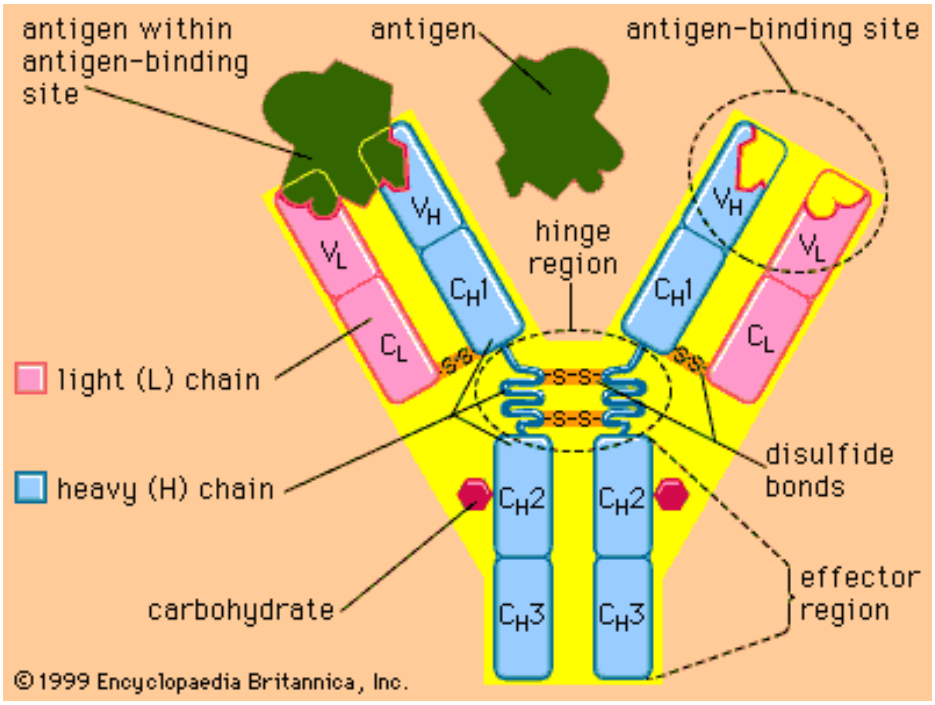

Figure 2-1. Basic antibody structure. Two identical heavy chains and two identical light chains are connected by disulfide bridges to form the antibody molecule.

and IgE as are illustrated in Figure 2-2 (Natvig and Kunkel, 1973). IgG is the most abundant antibody in serum. It is a monomeric antibody molecule consisting of two heavy and two light chains. In mice, four isotypes exist within the IgG class which are named IgG1, IgG2a, IgG2b and IgG3 (Mestas and Hughes, 2004). Each of these istotypes has a distinct function as determined by the Fc portion of the molecule (Spiegelberg, 1974). IgG1 and IgG3 are isotypes which can support antibody-dependent cellular toxicity and complement-dependent cytotoxicity. When an antibody is bound to a cell surface, the Fc region of the antibody and the Fcγ receptors on the immune effector cells such as neutrophils, macrophages and natural killer cells interact to cause cell death (Carter, 2001). The specificity for antigen is not affected by the class or isotype of the antibody. Any class and isotype of antibody could be specifically constructed for an invading antigen. IgA is a monomeric antibody for which only one isotype exists in mice, versus two in humans (IgA1 and IgA2). IgA is secreted in mucosal surfaces. IgM antibodies are the first to be produced after the initial contact with antigen. These molecules are pentameric, and therefore contain 10 heavy chains and 10 light chains. IgD has a monomeric antibody structure which functions as an antigen receptor for B cell induction. IgE is also a monomeric antibody structure and is involved in the allergy and asthma responses.

Before a B cell is activated by its cognate antigen, it does not secrete antibodies. When the B cell binds its cognate antigen with its surface IgD or IgM B cell receptor antibodies, and a co-stimulation signal is provided by a helper T cell the B cell will become activated to continue producing antibody (Reinherz et al., 1980). Once activated, a B cell will produce the default IgM antibody class unless the cell takes the opportunity to switch the (Fc) constant region class to IgG, IgA, or IgE. This class switching determines how the antibody will function as indicated in Table 2-1.

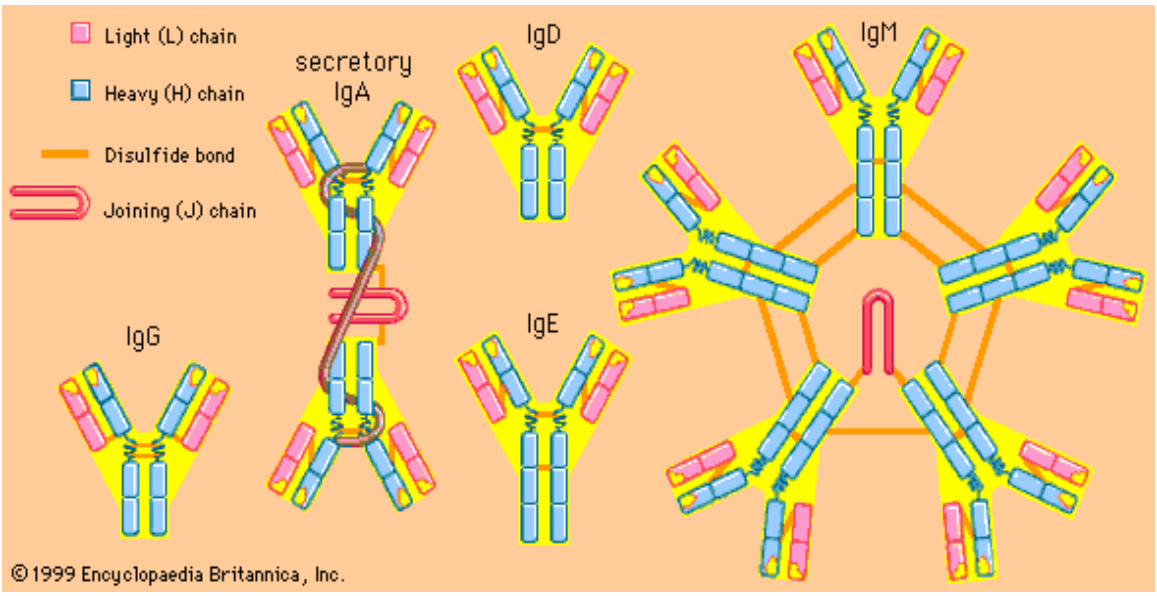

Figure 2-2. The five antibody classes

Table 2-1. Antibody class and functional properties defined by the Fc region

Antibody Class	**Functional Properties**
IgM	Fixes complement Opsonizes target antigens First antibody produced
IgA	Resistant to stomach acid Protects mucosal surfaces Secreted in milk
IgG	Fixes complement Opsonizes target antigens Assists NK cells to kill Crosses the placenta
IgE	Defends against parasites Causes anaphylactic shock Causes allergies
IgD	Antigen receptor for B cell induction

Antibody diversity is one of nature's masterpeices. The number of antigens an individual may encounter throughout their lifetime is unimaginable. Each antigen may be 'seen' differently by each genetic individual; the antigenic epitopes to which antibodies are made to be specific can differ greatly from individual to individual. An epitope is the specific antigenic site which the antibody will bind. Techniques such as limited proteolysis, epitope footprinting, epitope excision, epitope extraction and mass spectrophotometry are able to determine the Fab binding space (footprint) relative to the antigenic epitope (Hager-Braun and Tomer, 2005). Generally, epitopes can be 8-22 a.a. depending on the nature of the antigen and can bind to linear or folded conformations of a.a. With the knowledge that there are 20 a.a., there would therefore be a total of 20 billion combinations for an epitope of only 8 a.a. (Dreyer and Bennett, 1965). So, how do B cells have a diversity of this magnitude available for the creation of antibody molecules?

B cells undergo clonal selection and modular design to create such diversity. Clonal selection refers to the ability of one B cell to only make antibodies of one antigenic epitope specificity called its 'cognate antigen'. Modular design refers to the ability of the adaptive immune system to make a myriad of antibodies from different B cells when needed. Several genetic mechanisms appear to contribute to the generation of an indiviual's total repertoire of antibody specificites. B cells contain DNA which is specifically processed to create antibodies. This provides the basis for such enormous diveristy with respect to antigen specificity (Tonegawa et al., 1977). Firstly, both heavy and light chain genes utilize multiple alternative gene segments to assemble a complete variable region. Light and heavy chain assembly is a proccess which is generally explained as variable (V), joining (J), constant (C) recombination and V, diversity (D), J, C recombination, respectively (Schatz, 2004).

Antigenic challenge leads to rapid production of low affinity antibodies. It involves the proliferation of B cells drawn from a repertoire already available at the time of immunization. The potential repertiore is huge, but at any given time, only a fraction of the potential repertoire is available through a limited number of clones expressing specific antibodies. The generation of antibody diversity is further processed by somatic mutation. This produces high affinity antibodies, starting with the genes used in the first stage cells (Bothwell et al., 1981). Hypermutation of these genes is followed by antibody produced with increased affinity. The rate of mutation can reach 0.01 mutations per base pair per cell division (Kocks and Rajewsky, 1989).

2.4 Mab methodology

Monoclonal antibodies (Mabs) are defined as a population of antibodies with single antigenic epitope specificity. In 1975, Kohler and Milstein discovered that they could fuse B cells from an immunized mouse spleen to B cell myeloma cells to create hybridoma cells with immortal characteristics capable of secreting antibody of a single antigenic specificity. This began the Mab revolution. Mabs have become exceptional tools for molecular biology, biochemistry and medicine. The mechanism of fusion between these two cell types is understood as a plasma membrane fusion in the presence of polyethylene glycol. This creates a heterokaryon that possesses two or more nuclei. At the first cell division, the nuclei of the two originating cells fuse and a hybrid cell results. To select for growth of only the hybridoma cells, the use of myeloma cells incapable of producing purines and pyrimidines is used. Myleoma cell lines were created that were deleted for the enzymes thymidine kinase, hypoxanthine guanine phosphoribosyl transferase which are subsequently unable to synthesize DNA through salvage pathways. Additionally, in the presence of the folic acid antagonist aminopterin

(A) the main biosytheic pathway for purines and pyrimidines is blocked. Hypoxanthine and thymidine are intermediates in DNA synthesis. Hypoxanthine and thymidine are a purine derivative and a deoxynucleoside, respectively. The B cells from immunized mice provide functioning copies of the genes that encode the enzymes thymidine kinase and hypoxanthine guanine phosphoribosyl transferase. Consequently, in a media containing hypoxanthine, aminopterin and thymidine (HAT) a myeloma cell can be 'rescued' by fusion with a B cells which has the ability to produce DNA (Littlefield, 1964). Therefore, hybridoma fusions are grown in HAT medium to select for single antigen-specific antibody-secreting immortal hybridoma cells. Myeloma cell lines which do not secrete antibodies have been developed for use in monoclonal fusions. FO cells are commonly used for hybridoma fusions (de StGroth and Scheidegger, 1980). There would be a maximum of ten possible unique combinations of heavy and light chains, which could be used to produce an antibody molecule, if the myeloma cell line used for a fusion had the ability to produce antibody. Therefore, FO cells have been genetically modified so they do not produce antibody on their own.

Fusions should generally be done approximately four days after a final immunization with the antigen of choice. The reason for this is that recently activated B cells will fuse preferentially and will continue to secrete antibody once fused. Early after fusion, hybridoma cells are considered genetically unstable and may lose chromosomes. To support hybridoma cells, macrophages can be used to stabilize growth by providing growth factors and association properties. Generally, after seven to ten days, macroscopically visible colonies are formed which originated from a single hybridoma cell following the fusion. Screening of the supernatant from these hybridoma clones against the immunizing antigen allows selection of hybridomas which secrete a Mab able to bind to the antigen of interest.

2.5 Monoclonal versus polyclonal antibodies

The discovery of a method for fusion between normal antibody producing cells and murine myeloma cells to produce B cell hybridomas (Kohler and Milstein, 1975), presented an important immunological advance. Before this discovery, polyclonal serum was only antibody option available for scientists. Polyclonal antiserum is a mixture of antibodies produced by thousands of different B cell plasma clones. Polyclonal antiserum may additionally contain antibodies specific for surplus antigens, such as impurities in the immunizing antigen. However, some possible advantages of polyclonal serum are the low production costs, higher affinity, a spectrum of specific binding epitopes and a mixture of antibody classes. Whereas, some advantages of monoclonal antibody technology are the indefinite supply of antibody with defined properties, the specificity for a single epitope, rapid binding to antigen, the large amount which can be produced and purified. In order to obtain antibodies capable of differentiating Uev1A from Mms2, this Master's work has employed Mab technology.

2.6 Rationale for the development of Mabs specific to Uev1A

The objective of this research was to obtain Mabs capable of recognizing Uev1A, but not Mms2. These are located in the 30 a.a. N terminal sequence, a.a. 104, the 14 a.a. core region within a.a.116-129 (7/14 variable) and the four a.a. C-terminal sequence (2/4 variable). Hybridoma technology was the method of choice for this Master's research project for many reasons. Firstly, a pharmaceutically relevant molecule capable of distinguishing between these two proteins could be used as a putative inhibitor of Uev1A in cancer therapy. Secondly, the necessary equipment, cell lines and expertise from Dr. Barry Ziola to perform this methodology were readily available. Thirdly, hybridoma cell lines are generally able to provide Mabs of unlimited potential due to the immortal

phenotype of these cells; Mabs are naturally stable biological molecules. Fourthly, a molecule capable of differentiating between Uev1A and Mms2 has been sought after for many years and it was expected that Mabs would have the most success as this methodology has been well established. Finally, immunization of an individual can increase the number of autoantibodies as the individual ages (Yang et al., 1996). Autoreactive antibodies may be produced by memory B cells that survive the aging process and either become re-stimulated later in life or become no longer able to established tolerance mechanisms (Stacy et al., 2002). Thus, it would be expected that Mabs could be produced to both the unique human Uev1A epitopes as compared to mouse Uev1A and, to the regions of these proteins that are identical.

Many cancers have been treated with Mabs to target the translated product of a specific proto-oncogene. This is discussed in Chapter Five. If a Mab capable of recognizing the unique regions of Uev1A could be obtained, it would be of immense significance for not only molecular biology and biochemical research, but also as a possible cancer therapy or diagnostic tool. This is a challenging task from which the outcome may instigate many novel discoveries.

CHAPTER THREE

MATERIALS AND METHODS

Compositions of solutions, buffers, and media are given in Appendix A, and sources of DNA, plasmids, chemicals, equipment, supplies and computer programs are given in Appendix B

3.1 Molecular biology techniques

3.1.1 Plasmids and DNA

3.1.1.1 *UEV1A* and *UEV1B*

The glutathione-S-transferase (GST)-Uev1A and GST-Uev1B proteins were made from PCR-amplified cDNA clones of *UEV1A* (Deng et al., 2000) and *UEV1B* (Rothofsky and Lin, 1997). The amplified fragments were cloned into pGEX-6P (GE-Healthcare) to form N-terminal gene fusions to GST named pGEX-Uev1A and pGEX-Uev1B, respectively.

3.1.1.2 *MMS2*

The GST-Mms2 protein was made using the open reading frame (ORF) from previously reported isolation of cDNA clones (Broomfield et al., 1998). The ORF was PCR-amplified as a *Bam*HI-*Sal*I fragment and cloned into pGEX-6P to form an N-terminal gene fusion to GST named pGEX-Mms2.

3.1.1.3 *UEV1A* derivatives

The GST-Uev1AΔ1-10 protein was constructed by cloning a polymerase chain reaction (PCR)-amplified *UEV1A*30-510 as a *Bam*HI-*Sal*I fragment into pGEX-6P to form an N-terminal gene fusion to GST. The forward primer sequence was 5'CCCGGAT CCCTGAAGTCACAAAGC-3'. The reverse primer sequence was 5'-GGCGTCGACTTAATTGCTGTAACACTGTCC-3'. The final construct was named pGEX-Uev1AΔ1-10.

The GST-Uev1AΔ1-30 protein was constructed by cloning a PCR-amplified *UEV1A*90-510 as a *Bam*HI-*Sal*I fragment into pGEX-6P to form an N-terminal gene fusion to GST. The forward primer sequence was 5'-GCCGGATCCAT GGCCATCACCACAGGAGTAAAAG-3'. The reverse primer sequence was 5'-GGCGTCGACTTAATTGCTGTAACACTGTCC-3'. The final construct was named pGEX-Uev1AΔ1-30.

The GST-Uev1AΔ1-30,Δ110-130 protein was constructed using a megaprimer strategy employing two rounds of PCR (Tyagi et al., 2004). Figure 3-1 illustrates the PCR methodology for this construct. Using GST-*UEV1A*Δ1-89 as the template, the first round of PCR amplified nucleotides 297-510 with the forward primer annealing to nucleotides 297-330 and 392-426, thus deleting nucleotides 331-391. The forward primer sequence was 5'-TTTAACAAAACTAGCAAAATGG-3'. The reverse primer sequence was 5'-GGCGTCGACTTAATTGCTGTAACACTGTCC-3'. The second round of PCR used an *Eco*RI digested *UEV1A*Δ1-89 gene as one template and the megaprimer (product from round one). The forward primer sequence used was 5'-GCCGGATCCATGGCCATCACCACAGGAGTAAAAG- 3'. The reverse primer sequence used was 5'-GGCGTCGACTTAATTGCTGTAACACTGTCC-3'. The resultant PCR fragment containing nucleotides 90-330 and 392-510 was digested as a

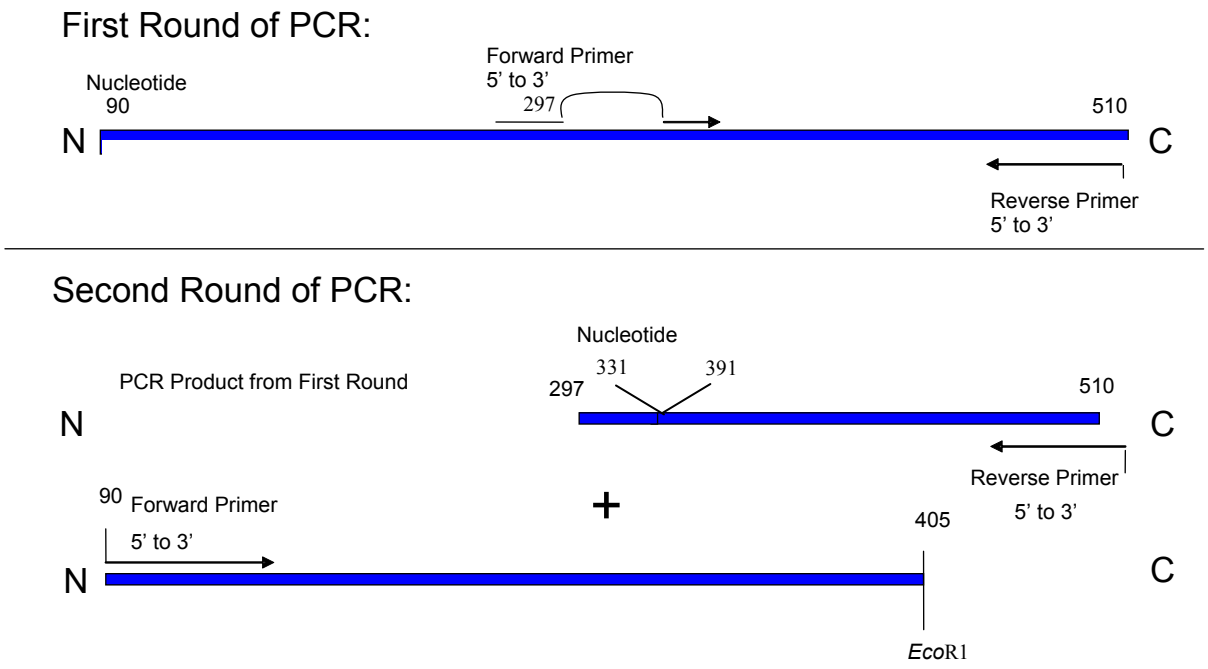

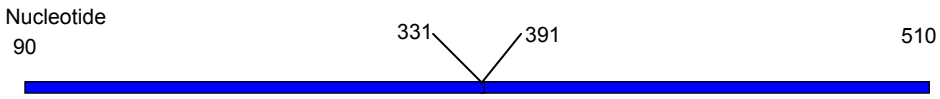

Figure 3-1. Polymerase chain reaction for core deletion mutants of Uev1A. Using *UEV1A*Δ1-89 as a DNA template, two primers were used to amplify the core-deleted megaprimer. The megaprimer contained nucleotides 90-330 and 392-510, and was further used to amplify an *Eco*R1-digested fragment of *UEV1A*Δ1-89. Amplification of *Eco*RI-digested *UEV1A*Δ1-89 and the megaprimer using forward and reverse primers, respectively, produced the final *UEV1A*Δ1-89, Δ332-390 construct.

*Bam*HI-*Sal*I fragment and cloned into pGEX-6P to form an N-terminal gene fusion to GST. The final construct was named pGEX-Uev1AΔ1-30,Δ110-130. Figure 3-1 illustrates the PCR methodology for this construct.

The GST-Uev1A44 protein was constructed by cloning a PCR-amplified *Bam*HI-*Sal*I-digested fragment containing nucleotides 1-132 into pGEX-6P to form an N-terminal gene fusion to GST. The forward primer sequence used was 5'-CCGGATCCATGCCAGGAGAGGTTCAAG-3'. The reverse primer sequence used was 5'-CCCCAGCTGCTCAAGAAGGTTGTC-3'. The final construct was named pGEX-Uev1A44.

The GST-Uev1A Δ1-30F104S protein was made using two rounds of PCR (see Figure 3-1 for the approach). GST-*UEV1A*Δ1-89 was used as the template for the first round of PCR in order to amplify nucleotides 294-510 coding region. The forward primer sequence was 5'-ACCCAGAAGCACCCCCTTTGTAAGATTTG-3' which contained the F104S megaprimer a.a. point mutation, thus changing it to Ser as seen in the Mms2 sequence. The reverse primer sequence was 5'-GGCGTCGACTTAATTGCTGTAACACTGTCC-3'. The second round of PCR used an *Eco*RI-digested *UEV1A*Δ1-89 gene as one template and the megaprimer as the second. The forward primer sequence used was 5'-GCCGGATCCATGGCCATCACCACAGGAGTAAAAG-3'. The reverse primer sequence used was 5'-GGCGTCGACTTAATTGCTGTAACACTGTCC-3'. The resultant PCR fragment was digested as a *Bam*HI-*Sal*I fragment and cloned into pGEX-6P to form an N-terminal gene fusion to GST. The final construct was named pGEX-Uev1A Δ1-30F104S.

The GST-Uev1A Δ1-30 +5 protein was constructed using two rounds of PCR (see Figure 3-1 for the approach). Using GST-*UEV1A*Δ1-89 as the template, the first round of

PCR amplified nucleotides 333-510. The forward primer sequence was 5'-AATATGAATGGAATAAA TAATTCCAGTGGGATGGTGGACCCA-3'. This primer sequence created point mutations inserting the Mms2 a.a. INNSS, therefore replacing the Uev1A a.a. VNSSN at a.a. 115-119. The reverse primer sequence was 5'-GGCGTCGACTTAATT GCTGTAACACTGTCC-3'. The second round of PCR used an *Eco*RI-digested *UEV1A*Δ1-89 gene as one template and the PCR amplified fragment as another template. The forward primer sequence used was 5'-GCCGGATCCATGGCCATCACC ACAGGAGTAAAAG-3'. The reverse primer sequence used was 5'GGCGTCGACTTAATTGCTGTAACACTGTCC 3'. The resultant PCR fragment containing nucleotides 90-510 with the point mutations at nucleotides 345-357 was digested as a *Bam*HI-*Sal*I fragment and cloned into the pGEX-6P to form an N-terminal gene fusion to GST. The final construct was named pGEX-Uev1AΔ1-30+5.

The GST-Uev1A Δ1-30+6 protein was constructed using two rounds of PCR (see Figure 3-1 for the approach). Using GST-*UEV1A*Δ1-89 as the template, the first round of PCR amplified nucleotides 360-510. The forward primer sequence was 5'-CTAATGGAGTGGTGGACGCCCG GAGCATACCAGTGCTAGCAAAA-3'. This primer sequence forced a sequence of point mutations inserting the Mms2 a.a. ARSIPV replacing the Uev1A a.a. PRAISV at a.a. 125-130. The reverse primer sequence was 5'-GGCGTCGACTTAATTGCT GTAACACTGTCC-3'. The second round of PCR used an *Eco*RI-digested *UEV1A*Δ1-89 gene as one template and the PCR-amplified fragment as another template. The forward primer sequence used was 5'-GCCGGATCCATGGCCATCACCACAGGAGTAAAAG-3'. The reverse primer sequence used was 5'-GGCGTCGACTTAATTGCTG TAACACTGTCC-3'. The resultant PCR fragment containing nucleotides 90-510 with the point mutations at nucleotides 375-390 was digested as a *Bam*HI-*Sal*I fragment and cloned into pGEX-6P to

form an N-terminal gene fusion to GST. The final construct was named pGEX-Uev1AΔ1-30+6.

3.1.2 Polymerase chain reaction

PCR was used to amplify DNA fragments for the purposes of cloning and deletion analysis of Uev1A. Reactions were carried out in a PTC-100 programmable thermal controller was used as the thermocycler to carry out the various reactions above. As a program guideline, a denaturing temperature of 95ºC for one min was followed by an annealing temperature of 48ºC for 30 sec, and primer extension was carried out at 72ºC for one min. These three steps were repeated 30 times per reaction.

3.1.3 pGEX-6P GST fusion vector

The pGEX-6P vector offers a *tac* promoter for chemically inducible, high level expression of the protein of interest. Overexpression is inducible with isopropyl-β-D-thiogalactopyranoside (IPTG) for *tac* promoter transcription of the GST-fusion gene. Uev1A, Uev1AΔ1-10, Uev1AΔ1-30, Uev1AΔ1-30,Δ110-130, Uev1A44 and Mms2 were cloned into *Bam*HI-*Sal*I restriction sites. Fusion proteins were purified from bacterial lysates by affinity chromatography using a Gluathione Sepharose 4B prepacked 5 ml column. Uev1A, Uev1AΔ1-30, Mms2 were cleaved using the PreScission Protease enzyme which cleaves the protein of interest from GST between Gln and Gly as seen in Figure 3-2.

3.1.4 DNA sequencing

DNA sequences were confirmed by automated DNA sequencing at the Plant Biotechnology Institute, Saskatoon, SK. All constructs sequenced used forward and reverse primers to the pGEX-6P plasmid which were named pGEX5' and pGEX3',

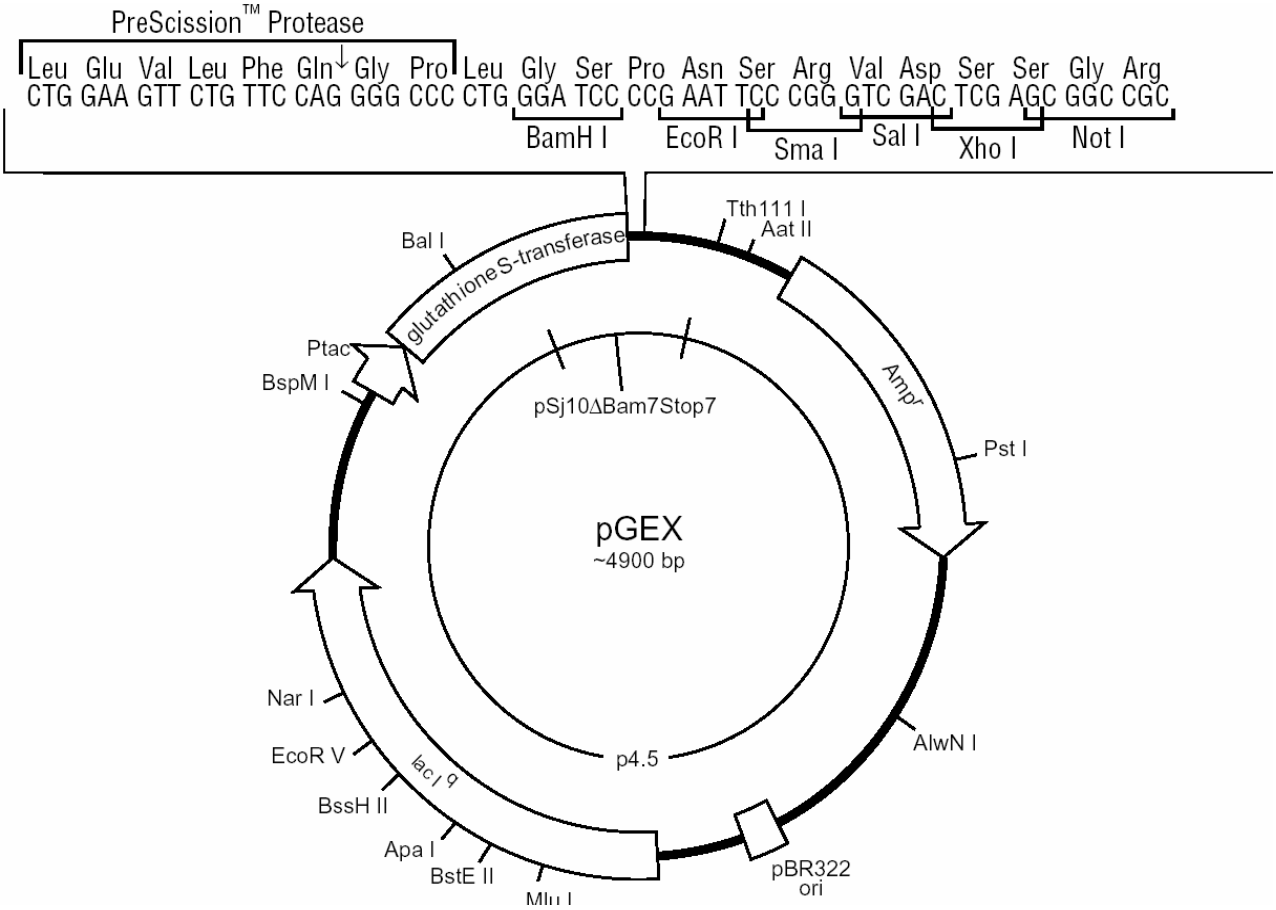

Figure 3-2. pGEX-6P cloning vector. The map of the GST-fusion vector shows the open reading frame and main features. Overexpression of a GST-fused protein of interest is inducible with IPTG for *tac* promoter transcription. pGEX-6P has a PreScission Protease cleavage site as shown between the Gln and Gly. All inserts were cloned into the *Bam*HI- *Sal*I restriction sites of pGEX-6P. This plasmid contains an ampicillin resistance gene **(**GE Healthcare**)**.

respectively. pGEX5' primer sequence is 5'-CTGGCAAGCCACGTTTG-3' and pGEX3' primer sequence is 5'-GGAGCTGCATGTGTCAG-3'. Sequences were further examined for the intended deletions and point mutations by nucleotide sequence alignment with the wild type gene.

3.1.5 DNA gel electrophoresis

Plasmid DNA and DNA fragments were separated by agarose gel electrophoresis. Gels of 0.6% agarose were loaded into an electrophoresis apparatus filled with 1X TAE buffer and a current of <100 mA was allowed until the proper migration distance was attained. Gels were stained in 0.5 μg/ml ethidium bromide for 5-10 min and the DNA was viewed using a UV trans-illuminator.

3.2 Recombinant protein expression and purification

3.2.1 Bacteria

The bacterial strain used in this study for protein expression was BL21-CodonPlus (DE3)-RIL [F- *ompT hsdS*(rB- mB-) *dcm*+ Tetr *gal*λ (DE3) *endA* Hte (*argU ileY leuW* Camr)]. This strain carries extra copies of the *arg*U, *ile*Y and *leu*W tRNA genes to help overcome codon bias. For plasmid DNA propagation and isolation, *Escherichia coli* DH10B (F- *mcr*A (*mrr-hsd*RMS-*mcr*BC) 80*lac*ZM15 *lac*X74 *rec*A1 *end*A1 *ara*139 (*ara*, *leu*)7697 *gal*U *gal*K - *rps*L (StrR) *nup*G) was used. With the exception of the incubation temperatures used for protein expression (see below), bacterial cells were incubated at 37°C. Bacteria cultures were grown in Luria Broth (LB). LB agar plates were prepared by the addition of water to a stock powder which was then autoclaved, cooled to 55°C, and poured into Petri plates. When plasmid selection was required, media was cooled to 55°C and supplemented with ampicillin to a final concentration of 50 μg/ml.

3.2.2 Bacterial transformation

Transformation of competent bacterial cells was performed by electroporation. For an electroporation, 25 µl of competent DH10B cells, stored in aliquots at -70°C, were placed on ice to thaw. Approximately 0.1 µg of plasmid DNA was added to the cells and allowed to incubate on ice for 45 sec. This plasmid and cell mixture was transferred to a cold Gene Pulser Cuvette that was then loaded into a Bio-Rad *E. coli* Gene Pulser and administered a 1.80 kV electric pulse. The electroporated cells were suspended into 400 µl of SOC liquid media and were subsequently incubated in a 37°C incubator for 45 min. Half of the cell suspension was then spread evenly onto an appropriate selectable agar plate for an overnight incubation at 37°C. Putative transformants were streaked onto selective medium prior to their experimental use. For short-term storage, the bacterial cell plates were sealed and then placed at 4°C for up to one month. For long-term storage, actively growing bacterial cultures were suspended in 10% dimethyl sulfoxide and then frozen and stored at -70°C indefinitely.

3.2.3 Recombinant protein overexpression

BL21(DE3)-RIL cells transformed with pGEX-MMS2, pGEX-UEV1A, pGEX-Uev1AΔ1-10, pGEX-Uev1AΔ1-30 pGEX-Uev1AΔ1-30Δ110-130, pGEX-Uev1A44 , pGEX-Uev1AΔ1-30F104S, pGEX-Uev1AΔ1-30+5, pGEX-Uev1AΔ1-30+6 and pGEX-Uev1B were grown overnight at 37 °C in LB + amp media and then sub-cultured 1:50 into 37°C LB + amp the following day. Cells were allowed to grow to an optical density (OD) at 600 nm of between 0.6 and 0.8, and were then induced with 0.5 mM IPTG at 37°C for 2 hours. Cells were harvested by centrifugation at 10,000 rpm in an Avanti Beckman JA10.5 rotor and resuspended in phosphate-buffered saline (PBS).

3.2.4 Preparation of cell extract

Crude cell extracts, from bacterial overexpression of our protein of interest, were kept at 4ºC and were passed through a French Press at 10,000 psi. The soluble fraction was retained after centrifugation at 17,000 rpm in an Avanti Beckman JA17 rotor for 30 min. The soluble fraction was then run through a chromatography system for purification.

3.2.5 Chromatography

Soluble cell extracts were passed through a pre-packed 5 ml GSTrap column, which was then washed with 5 column volumes of 1X PBS. GST-fusion proteins were eluted from the column with reduced glutathione elution buffer. The purified proteins were then dialyzed into cleavage buffer and concentrated in Amicon Ultra centrifugal 54 filter devices. When needed, cleavage from GST was performed by the addition of 1 µl of prescission protease per 400 µg of fusion protein, followed by overnight incubation at 4°C with gentle rocking. Cleaved proteins were then run through the GSTrap column in order to remove the GST from the cleaved protein of interest.

3.2.6 Protein analysis

3.2.6.1 Protein concentration

Protein concentrations were determined by using the BCA Protein Assay Kit as per the instruction manual. Purified proteins were kept at -20°C for short-term use, or were frozen in 1 ml aliquots and kept at -70°C for long-term storage.

3.2.6.2 SDS-PAGE

Proteins were visualized using sodium dodecyl sulfate polyacrylamide gel electrophoresis (SDS-PAGE) in the Mini-Protean 3 gel apparatus. Protein samples were

prepared at a 1:2 dilution into protein sample buffer. The protein samples were placed in boiling water for 5 min and loaded onto the protein gel. Gels were used at a 12% discontinuous (5% stacking, 12% separating) Tris-glycine polyacrylamide (37:1 acrylamide: bisacrylamide) concentration. This recipe can be found in the Molecular Cloning Laboratory Manual (Sambrook et al., 1989). Gels were stained with Coomassie Blue staining solution for at least 30 min, followed by incubation in de-stain solution until appropriate protein band could be visualized (after 30 min-1 hr).

3.2.6.3 Western blotting analysis

Following SDS-PAGE, the separating gels were equilibriated for 20 min in transfer buffer along with equal-sized polyvinylidene difluoride (PVDF) membranes and 3M filter papers. The components were assembled as described in manual for the Bio-Rad trans-blot semi-dry transfer cell, which was used for the transfer of proteins onto the PVDF membranes. Transfers were performed at a constant current of 1 mA/cm^2 for 2 hr. Membranes were then incubated in a blocking solution overnight at 4°C. The primary antibody was diluted in 10 ml PBST and incubated with the membranes at room temperature (RT) for 1 hr with gentle rocking. The membranes were washed 3 times for 5 min each with PBST. The rabbit-anti-goat IgG heavy and light chain alkaline phosphastase-conjugated and goat-anti-mouse IgG heavy and light chain alkaline phosphastase-conjugated secondary antibodies were diluted at 1:2,000 in 10 ml PBST and incubated with the membranes as with the primary antibody. The membranes were then washed 3 times for 5 min each with PBS to prepare for detection. The detection of alkaline phosphatase-conjugated secondary antibodies was performed by a colorimetric reaction using the substrates nitroblue tetrazolium chloride and 5-bromo-4-chloro-3-

indolyl phosphate diluted in alkaline phosphatase buffer to 330 µg/ml and 165 µg/ml, respectively.

3.3 Preparation for hybridoma fusions

3.3.1 Mouse immunizations

Experimental procedures using BALB/c mice were approved by the University of Saskatchewan Committee on Ethics in Animal Experimentation. Mice were cared for as prescribed by the Canadian Council on Animal Care Guidelines. Mice were immunized intraperitoneally with 35 µg of purified antigen, in PBS, emulsified in Freund's incomplete adjuvant, with the emulsion then dispersed into equal volume of PBS containing 2% Tween 80 immediately prior to injection (Herbert et al., 1965). Mice were boosted three times following initial immunization. For each boost, 17.5 µg of purified antigen was similarly prepared as above. The first boost was administered 33 days after the initial immunization. The second boost was administered 57 days after the initial immunization. The third boost was administered 100 days after the initial immunization. The process is depicted in Figure 3-3.

3.3.2 Preparation of polyclonal serum

Polyclonal sera were obtained via tail bleeding of the immunized mice at various times following immunization with purified antigen. Using a razor blade, a small cut was made along the underside of the tail vein. Blood was placed a 4ºC for three hr. At that time, the blood sample was centrifuged for two min at 13,000 rpm. Serum was transferred to a new eppendorf tube (E-tube) and stored at -20ºC until tested for reactivity to the immunizing and other antigens (see Section 3.5.1).

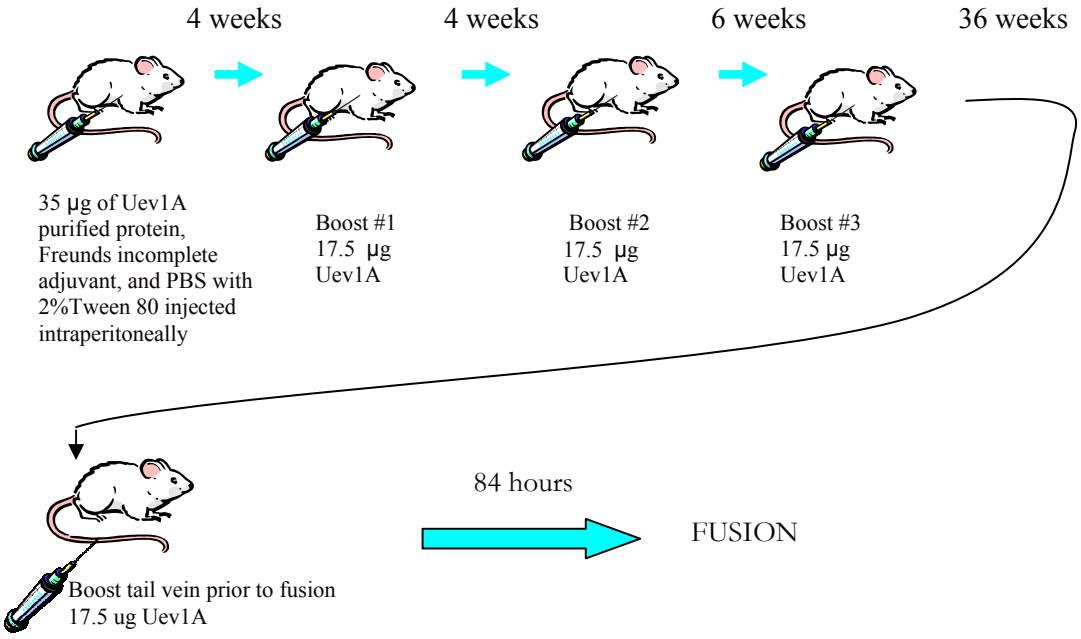

Figure 3-3. Timeline of mouse immunizations prior to hybridoma fusion. Each mouse was administered the Uev1A antigen intraperitoneally, except for the final boost which was given via a tail vein. Each mouse was boosted 4 times, over the period of one year, prior to the hybridoma fusion.

3.3.3 Pre-fusion boost

Four days prior to the hybridoma fusion, 354 days after the initial immunization, 17.5 μg of purified antigen in PBS was injected into the tail vein.

3.4 Hybridoma fusions

3.4.1 Harvesting of macrophages

Four BALB/c mice were sacrificed by cervical dislocation and washed with 70% ethanol. The mice were set onto their back and a small incision was made near the middle of the abdomen. The skin was then separated half towards the head and half towards the tail. A needle was inserted under the abdominal wall and five mls of 0.34 M sucrose was injected into the abdominal cavity. The sucrose was then drawn back into the syringe and this process was repeated three times. The macrophages suspended in the sucrose were then collected by centrifugation at 700 X g for 5-8 min. The supernatant was removed and the pellet was resuspended into 100 ml of 1640 HAT media. The macrophages were then plated into ten 96 well tissue culture plates to be used as feeder cells for the B-cell hybridomas.

3.4.2 Hybridoma growth media and selection

The main biosynthetic pathway for purines and pyrimidines is blocked by the a.a. antagonist aminopterin. In the presence of aminopterin, cells which still have endogenous thymidine kinase and hyoxanthine quanine phosphoribosyl transferase can continue to synthesize DNA through DNA salvage pathways. However, if either thymidine kinase or hyoxanthine quanine phosphoribosyl transferase is missing, DNA synthesis ceases. Spleen cells with thymidine kinase and hyoxanthine quanine phosphoribosyl transferase, which would die in culture after a few days, were fused to

myeloma cells lacking thymidine kinase and hyoxanthine quanine phosphoribosyl transferase. A single myeloma cell is subsequently rescued by a fusion with an immunized B cell which supplies the missing enzymes. Only the hybrid cells will grow in 1640 HAT medium which contains hypoxanthine, aminopterin, and thymidine.

3.4.3 Myeloma and immunized B cell fusion

3.4.3.1 Splenectomy

A Uev1A-immunized mouse was sacrificed by cervical dislocation and placed onto its right side in a sterile tray. The mouse was liberally washed with 70% ethanol. An incision was made posterior to the left side of the ribcage. The skin was separated and scissors and forceps were used to remove a large skin flap over the area of the spleen. The facia and musculature were opened and the spleen was removed and washed in a dish containing 10 ml of S-O media. The spleen was then placed into 3 ml of fresh S-O medium and the dish containing the spleen was transferred to a sterile biosafety cabinet. The spleen was poked full of holes with a 26 gauge needle and 5 ml of S-O media were gently forced through the spleen causing ejection of the spleen cells. This procedure was repeated again. The spleen cells are confirmed to be removed when the spleen color becomes relatively clear. The cells and medium were placed into a 50 ml tube and centrifuged at 900 X g for seven min. The supernatant was removed and the cell pellet was tapped loose in preparation for fusion with FO Myeloma cells.

3.4.3.2 Preparation of Myeloma cells for fusion

FO cells are permanently stored in liquid nitrogen. When needed, the FO cells were removed from the liquid nitrogen tank and warmed rapidly to 37ºC for two min. The cells were washed with 15 ml of S-10 medium and resuspended into 40 ml of S-10

medium. These cells were allowed to grow for approximately 5 days in preparation for fusion with the Uev1A-primed B cells from the splenectomy.

3.4.3.3 Hybridoma fusion

Two hybridoma fusions were concurrently performed, one by Dr. Barry Ziola and one by me. Each fusion used B cells from a separate Uev1A-immunized BALB/c mouse. S-O serum-free medium was used to mix 10^8 spleen cells and 2 X 10^7 myeloma cells. The cells were centrifuged for eight min at 400 X g and the supernatant was completely removed. The pellet was broken by gently tapping the bottom of the tube. Fusions were performed in a 37ºC waterbath for the remainder of the protocol. One ml of 50% PEG, pre-warmed to 37ºC, was added to the pellet over a period of one min, with continual stirring. Stirring of the cells was continued for two additional min. Fourteen ml of S-O medium were then added slowly over fourteen min with continual stirring. The cells were incubated for 5 min and subsequently centrifuged for eight min at 400 X g. The supernatant was discarded and the pellet was resuspended into Rosewell Park Memorial Institute medium (RPMI) 1640 HAT selection media in ten 96 well tissue culture plates. The hybridoma cells were monitored for seven days, the medium was changed upon first observation of acidic pH adjustment in the media color and the cells were tested for Mab specificity to Uev1A after at least 25% confluency was reached.

3.5 Hybridoma screening

3.5.1 Enzyme immunoassays

High protein binding Immulon 4 flat-bottomed, 96 well plates were used in all enzyme immunoassays (EIA)s. Antigen was plated at 0.5 μg in 100 μl of PBS per well and allowed to bind the plate overnight at RT. The plate was then emptied and

unadsorbed antigen was removed by inverting the plate and tapping on paper towel. The primary antibody was added using a dilution series or at a predetermined dilution in assay diluent. Following a one-hr incubation at 37ºC, the primary antibody was dumped out and the plate was washed again four times with rH_20 followed by tapping on paper towel between each wash. The horseradish peroxidase (HRP)-conjugated secondary antibody was added at a predetermined dilution in 100 µl of EIA assay diluent per well. Following one-hr incubation at 37ºC, the secondary antibody was dumped and the plate was washed four times in rH_20. A tetramethylbenzidine microwell peroxidase substrate was used to develop a deep blue color when reacted with HRP. The plate was allowed to develop for 30 min in the dark after which 1 M phosphoric acid was added to stop the reaction. The acid turned the TMB substrate yellow and the reaction was read at a wavelength of 450 nm in an EIA reader using MacReader 2.0 Software.

When polyclonal antiserum was assessed for antibody by EIA, a mathematical approach was used to determine the level (titer) of antibodies able to bind a given antigen. Four EIA data points were used, with the antibody dilutions involved being those successive two-fold dilutions that gave EIA results above and below $OD_{450nm} = 0.5$. Reciprocals of the antiserum dilutions were converted to $\log_{10}$ values and a straight line equation was derived for these values and the associated EIA values. The equation was then used to determine the antiserum dilution that would give an EIA result of exactly 0.5. The reciprocal of this dilution was defined as the antiserum titer.

3.5.2 Ascites fluid production

Mabs of the desired binding specificity were subject to ascites production. The hybridoma cells producing Mab specific to Uev1A were grown in tissue culture in RPMI 1640 S-10 medium until approximately 70 percent confluency in a T75 Tissue culture

flask was reached. Growth of hybridomas in ascetic fluid of mice can produce from 1 to 10 mg/ml of Mab. Mice were injected intraperitoneally with 0.3 ml of Freund's incomplete adjuvant 24-48 hr prior to injection to help stimulate ascites formation. The hybridoma cells were collected by centrifugation and washed twice in 50 mls of RPMI. Approximately 10^6 hybridoma cells were resuspended in 2.5 mls of RPMI and were injected into the peritoneum of a BALB/c mouse. Ascites fluid was produced within seven to fourteen days. Ascites fluid was removed and the mice were sacrificed.

3.5.3 Isotyping

EIAs were performed using tissue culture supernatant containing Mabs produced by stable hybridoma cell clones. The 96 well EIA plate was coated with 0.75 μg per well of goat anti-mouse IgG + IgM heavy and light chain specific 'trap' antibody. This antibody was allowed to adsorb to the plate overnight at RT. Following removal of the unadsorbed antibody by tapping on paper towel, the tissue culture supernatant was added to each well at a 1:2 dilution in EIA assay diluent in a final volume of 100 μl per well. After 1 hr at 37ºC, the plate was emptied and washed four times in H_20 and then secondary antibodies were added. To discover the class and isotype of each Mabs, six secondary antibodies were used: anti-mouse IgGγ:HRP, anti-mouse IgG1:HRP, anti-mouse IgG2a:HRP, anti-mouse IgG2b:HRP and anti-mouse IgM:HRP. These secondary antibodies were tested in duplicate for reactivity with the Mabs. The plate was washed, then developed and read as stated in section 3.5.1.

3.6 Competition analysis

3.6.1 Horseradish peroxidase conjugation

HRP-conjugation was done according to a modification to the procedure of Nakane and Kawaoi (1974) whereby the blocking and molecular sieve chromatography steps were ommitted. Ascites fluid were diluted from 2 ml to 3.5 ml with PBS and placed at 4°C. While stirring for approximately 2 min, 3.15 mL of RT saturated ammonium sulphate solution was added dropwise. After 1 hr at 4°C, the mixture was centrifuged at 9,000 × *g* at 4°C for 10 min. The pellet was dissolved in 3.5 ml of 4°C PBS and the precipitation was repeated. Recovered antibody was dissolved in 3.0 ml of 4°C PBS and dialyzed for 2 days at 4°C against 300 volumes of 10 mM sodium carbonate (pH 9.5). Fresh buffer was used each day. Following dialysis, insoluble material was removed by centrifugation for 10 min at 850 × *g* at RT. Concentration of the clarified immunoglobulin solution was determined at 280 nm using an extinction coefficient of 13.0.

Five mg of HRP was dissolved in 1.0 ml of freshly made 0.3 M $NaHCO_3$. One ml of 0.08 M $NaIO_4$ was added and the contents were mixed gently for 30 min at RT. The mixture turned a green-yellow color. At this time, 1.0 ml of 0.16 M ethylene glycol was added and the contents were allowed to mix gently at RT for 1 hr. The solution was dialyzed against three 1 L changes of 0.1 M Na_2CO_3. At a 1:1 mg ratio, purified Mab was added to aldehyde-activated HRP and allowed to mix gently at RT for 2-3 hr. After this, equal mg weight of $NaBH_4$ was added and the solution was left to mix for 3 hr. The solution was then dialyzed against three 1 L changes of PBS at 4ºC. Merthiolate was added to 0.2 mM and the conjugates were stored at 4°C for the duration of the experiments.

3.6.2 Epitope mapping

3.6.2.1 Titration of HRP:Mab conjugates

The dilution of each conjugate giving a background-corrected $OD_{450\ nm}$ value of l.0 was determined by an EIA in 96 well Immulon 4 plates. Uev1A was allowed to bind the plate at a concentration of 0.5 μg in a dilution of 100 μl per well of PBS overnight at RT. Removal of buffer and unadsorbed antigen from each well was performed by inverting the plate and tapping on paper towel. Assay diluent (100 μl) was added into each well to block the plate. Dilutions of HRP–Mab conjugates were made in assay diluent and 100 μl of each dilution were added to four wells. After one hr at 37°C, the solution was dumped from the well and the wells were washed four times in RT rH_2O, followed by inversion and tapping of remaining fluid on paper towel. Each well received 100 μl of substrate solution. After 30 min at RT in the dark, 100 μl of 1 M phosphoric acid were added per well and the plates were read as described in section 3.5.1.

3.6.2.2 Mab competition EIAs

To determine whether an unconjugated Mab was able to inhibit the binding of an HRP-conjugated Mab, two EIAs were performed using the same Mab dilutions. Firstly, in a direct Mab binding EIA, 100 μl of each Mab dilution were added to a single well containing adsorbed Uev1A. The Mab dilution giving a background-corrected OD of 1.0 was found by linear interpolation, using the three dilutions yielding assay values closest to 1.0. In the second EIA, a Mab binding competition EIA, 100 μl of each Mab dilution was again added to a single well containing adsorbed Uev1A. Unlike the Mab direct binding EIA, however, the plates here were not dumped and washed after the initial 1 hr incubation at 37°C. Instead, 100 μl of HRP-conjugated Mab was directly added to each well, with the dilution used being that giving a final background-corrected $OD_{450\ nm}$ value

of 1.0 as determined by the titration EIA in section 3.6.2.1. Eight wells that received only assay diluent during both incubations were used to determine the assay background value for that plate. Similarly, for each plate, eight wells receiving assay diluent during the first incubation and diluted HRP-conjugated Mab during the second incubation were used to determine the background-corrected $OD_{450\ nm}$ value for 100% binding of the HRP-conjugated Mab. The dilution of unconjugated Mab which gave 50% inhibition of HRP-conjugated Mab binding was determined by interpolation using the three dilutions yielding inhibition values closest to 50%. Because Mabs in ascites fluid were used in these competition EIAs, the ability of each Mab to hinder binding of a given HRP-conjugated Mab was related to the Mab dilution that gave an assay background corrected $OD_{450\ nm}$ value of 1.0 in the direct Mab binding EIA. The following formulas were constructed to calculate the competition (Ziola et al., 1999).

$$\frac{\text{Reciprocal of dilution giving a direct binding EIA value of 1.0}}{\text{Reciprocal of dilution giving a competition EIA value of 50\%}} = \text{Competition index}$$

The competition index for each Mab was then related to the competition index for the Mab conjugated with HRP (i.e., the homologous Mab) according the following formula:

$$\frac{\text{Mab competition index}}{\text{Homologous Mab competition index}} = \text{Relative competion index}$$

By mathematical definition, the relative competition index for the unconjugated homologous Mab will be 1.0. Any Mab with a relative competition index much larger than 1.0 is considered to be unable to inhibit binding of the HRP-conjugated Mab. Any Mab with a relative competition index less than 1.0 is considered to have the capability,

based on binding topography, to compete with an HPR-conjugated Mab better than it can with its homologous HRP-Mab. For example, if one Mab is binding to a three dimensionally more topographically accessible distinct site, it can block the binding of an HRP-conjugated Mab which binds to a less topographically accessible distinct site. In this case, the unconjugated Mab would be capable of blocking the binding of the HRP-conjugated Mab better than it can block a Mab identical to itself; a relative competition index of less than 1.0 would result. Mab 2H11 was also used in the competition experiments. It is a Uev1A- and Mms2-binding Mab that originated in Dr. Wei Xiao's lab and was produced by Parker Andersen.

3.7 Formalin-fixed paraffin-embedded tissue immunohistochemistry

Paraffin blocks containing embedded tissue were cut to 4 micron thickness and then tissue sections were placed on positively charged slides. Normal thyroid tissue was used as a positive control for Uev1A staining based on a screen of mRNA by Northern blot (data not shown). Slides with unstained sections were stored at 4ºC if used immediately and at -70ºC for long term storage. Slides were prewarmed to RT and dried before they were baked at 60ºC overnight prior to the immunoassay. The slides were deparaffinized and rehydrated as follows: four 5 min washes in xylene, three quick washes in 100% ethanol, two quick washes in 95% ethanol and one 5 min wash in 70% ethanol. Following tissue-rehydration, heat-induced epitope retrieval was done by cooking slides in a microwave oven in 1 mM ethylenediamintetraacetic acid (EDTA) buffer at pH 9.0. Endogenous peroxidases were blocked in the tissue slides by incubating for 10 min in 3% hydrogen peroxide in methanol to reduce false-positive staining. The slides were rinsed in rH_2O three times for 5 min for rehydration and were then stored in rH_2O until the immunoassay was performed.

The formalin-fixed paraffin-embedded tissue slides were incubated with 200 µl of the primary antibody at a 1/50 dilution in immunohistochemistry antibody-dilution buffer. In addition, Mab LN1 antibody was also pre-absorbed by Uev1A protein by incubating the mixture for 12 hours prior to use with Uev1A protein at a concentration of 0.2 mg/ml. Both, Mab LN1 and Uev1A-preabsorbed Mab LN1 solutions were added to the respective slides and incubated overnight at 4ºC in a hydration chamber. Secondary antibodies reactions for visualization of the bound primary Ab were performed using the Envision Dako Kit. Slides were gently rinsed in PBS by placing them in a Coplin jar for three 5 min washes. Excess buffer was removed and slides were placed in a humidity chamber one at a time and dehydrated with three-four drops of HRP labeled secondary anti-mouse antibody solution. The solution was incubated at RT for 30 min. Slides were then rinsed and incubated with 200 µl of diaminobenzidine chromagen substrate for 10 min and rinsed with PBS. After rinsing, the slides were washed three times for 5 min in PBS. For color enhancement, subsequently the slides were incubated in a 2% copper sulphate solution for 5 min and then rinsed well with rH_2O. Slides were then dipped in Haematoxylin 1 fifteen times, and then washed in rH_2O until slides were completely clear, which was used as a counterstain to visualize the nuclei of the cells. Slides were immediately dehydrated for cover slipping as follows: three times in 95% enthanol, three times and 100% ethanol and four times in xylene. Slides were then stored in a final xylene wash and mounted one at a time using appropriately sized coverslips and 2-3 drops of cytoseal mounting solution (performed by Dr. Emina Torlakovic).

CHAPTER FOUR

RESULTS

4.1 Purified Uev1A, Uev1AΔ1-30 and Mms2 proteins

The central goal of this thesis research was to obtain Mabs capable of recognizing and distinguishing Uev1A from Mms2. In order to carry out the stated objective, purification of proteins of importance, namely, Uev1A and Mms2 was necessary. Genetic cloning of *MMS2* and *UEV1A* full length, deletion and mutational constructs into the pGEX-6P GST-fusion vector facilitated overexpression of the respective proteins for protein purification. Each inserted gene was constructed by PCR using the restriction sites *Bam*H1 and *Sal*1, and ligated into a *Bam*H1-*Sal*1-digested pGEX-6P vector as illustrated in Figure 3-2. Protein purification was performed using glutathione sepharose column chromatography and the resultant Mms2, Uev1A and Uev1AΔ1-30 proteins were obtained at high purity as shown in Figure 4-1. The GST-fusion protein was cleaved from these overexpressed proteins in the purification process.

4.2 Mouse immunizations and polyclonal antibody response to Uev1A and Mms2

Full-length Uev1A was used for immunization of BALB/c female mice over the course of one year. The mice were immunized a total of five times as can be seen in the timeline provided in Figure 3-3. Polyclonal serum was obtained and directly tested in an EIA against Uev1A and Mms2 antigens. At an OD_{450nm} of 0.5, titers of 275,000, versus 95,000, a 3-fold difference, was found for antibody binding to Uev1A and Mms2,

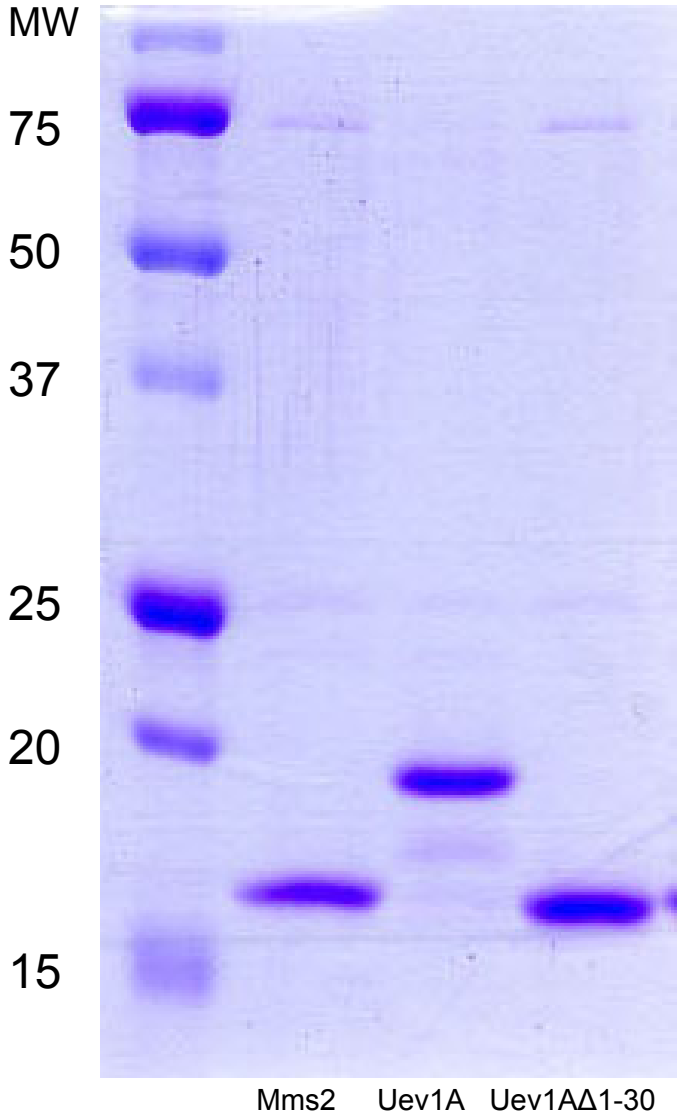

Figure 4-1. SDS-polyacrylamide gel of purified proteins Mms2, Uev1A and Uev1AΔ1-30. Mms2, Uev1A and Uev1AΔ1-30 were purified using GST-column chromatography to final GST-cleaved concentrations of 0.15 mg/ml, 0.2 mg/ml and 0.185 mg/ml, respectively. Ten microliters of each purified protein sample were analyzed. The gel was stained with Coomassie blue.

respectively. These results are presented in Figure 4-2. Additionally, response to any residual cleaved GST-impurities in the immunizing antigen proved to be negligible in line with the purity of the Uev1A antigen observed in Figure 4-1. The differential response observed provided confidence in the likelihood of producing Mabs specific to Uev1A. Consequently, Dr. Barry Ziola and I each performed a hybridoma fusion with one of the Uev1A-immunized BALB/c mice. In each fusion, the mouse spleen was removed and B cells were fused with FO Myeloma cells.

4.3 Mab binding to Mms2, Uev1A and Uev1AΔ1-30

Analysis of Mabs secreted in the supernatant of hybridoma cell growth medium was performed using EIAs. Nine hundred and sixty hybridomas were tested for a binding response to Uev1A and Mms2. Of these nine hundred and sixty hybridomas, twelve secreted Mabs capable of interacting only with Uev1A, while one secreted a Mab capable of interacting with both Uev1A and Mms2. Of the twelve Uev1A-specific Mabs, six interacted only with Uev1A and the other six interacted with both Uev1A and Uev1AΔ1-30. The immunoglobulin class for each of the original thirteen hybridoma clones is outlined in Table 4-1 along with the successfully recloned renamed hybridomas. Following selection using specific criteria, five Mabs were obtained and successfully recloned. IgM and mixed IgM/IgG Mabs were discarded from the Uev1A screen due to the IgM pentameric bulky structure. Six additional Mabs lost reactivity over the screening period. Four of the five remaining Mabs are specific to Uev1A and not Mms2, and the other Mab reacts with both. As shown in Tables 4-1 and 4-2, the five remaining Mabs have been renamed LN1, LN2, LN2A, LN2B and LN3. The original names of each hybridoma cell line are shown in Table 4-1 to provide a published link to the original raw data obtained.

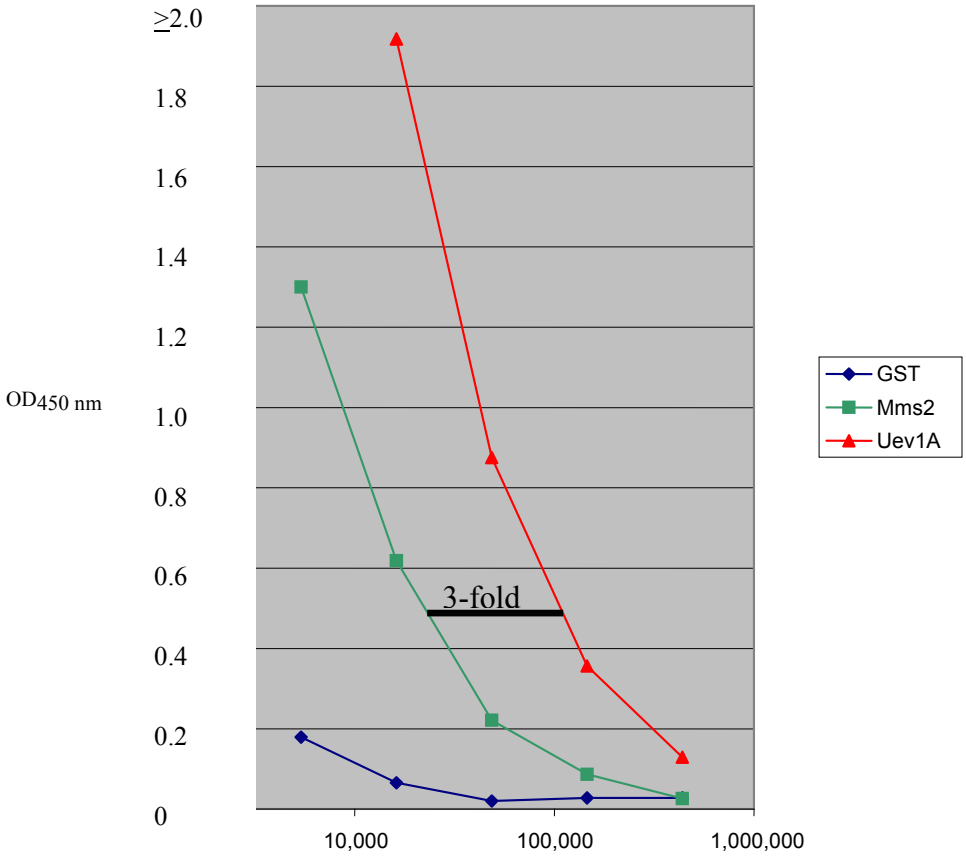

Figure 4-2. **Binding of anti-Uev1A polyclonal antibodies to GST, Mms2 and Uev1A.** The 3-fold higher reactivity to Uev1A demonstrates the putative antibody reactivity specific to the four unique regions of Uev1A.

Table 4-1. Antibody classes of hybridoma clones.

Original Name	New Name	Class
Z1-D8	-*	IgG
N3-E2	-	IgG and IgM
N1-E5	-	IgM
N1-H2-A6	LN2	IgG
Z4-F12	-	IgG
Z1-F3	-	IgG
Z1-F1	-	IgG
Z4-A8	-	IgG
Z4-D4-B3	LN2B	IgG
Z4-G7	-	IgG and IgM
Z1-B3-A11	LN1	IgG
N4-B4-B3	LN2A	IgG
Z5-D2-F12	LN3	IgG

*Dashed line represents the absence of a new name due to being unable to establish a stable recloned hybridoma cell line.

Table 4-2. Phenotypic interaction profiles of Mabs secreted by hybridoma cell lines.

Renamed Hybridoma Cell Lines	Uev1A	Uev1AΔ1-30	Mms2	Mab Isotype
LN1	+	-	-	IgG1
LN2	+	+	-	IgG2b
LN2A	+	+	-	IgG1
LN2B	+	+	-	IgG1
LN3	+	+	+	IgG2b

Using Uev1A, Uev1AΔ1-30 and Mms2 purified proteins, analysis was carried out to characterize binding to the N-terminal 30 a.a. of Uev1A as well as to observe a differential binding of Uev1A and Mms2. Figure 4-3, Figure 4-4 and Table 4-2 show that Mab LN1 binds to Uev1A, but not Mms2 or Uev1AΔ1-30, providing a possible Uev1A N-terminal specific antibody. Mabs LN2, LN2A and LN2B have been named because they all bind to Uev1A and Uev1AΔ1-30, but not Mms2, providing three possible core-specific Mabs. These three Mabs share the same antigen binding profile, but originated from independent hybridomas. Mab LN3 binds to all three antigens and therefore does not distinguish between Uev1A and Mms2.

4.4 Mab binding to Uev1A-deletions

In order to characterize the antigenic epitopes of Mabs LN1, LN2, LN2A, LN2B and LN3, deletion and mutational constructs of Uev1A were made by using PCR, site-directed mutagenesis and molecular cloning techniques. Using these constructs, the exact binding locations were determined due to a loss of binding when epitopes were deleted or mutated. These constructs included Uev1A44, Uev1AΔ1-10 and Uev1AΔ1-30Δ110-130. The a.a. sequence alignment and comparative sequence illustrations of these proteins are shown in Figure 4-5. These protein constructs were overexpressed in *E.coli* and used for Western blotting directly without further chromatography purification. As seen in Figure 4-6, Mab LN1 reacts with Uev1A, Uev1AΔ1-10, Uev1A44 but not Uev1AΔ1-30, Uev1AΔ1-30Δ110-130, Uev1B and Mms2, making it specific for a.a. 10-30 of Uev1A. Mabs LN2, LN2A and LN2B Mabs react with Uev1A, Uev1AΔ1-10, Uev1AΔ1-30 and Uev1B, but not Uev1A44, Uev1AΔ1-30Δ110-130 and Mms2, making them specific for the core a.a. 110-130 of Uev1A. Lastly, Mab LN3 reacts with all seven constructs, making it specific for a.a. 30-44 of Uev1A and Mms2.

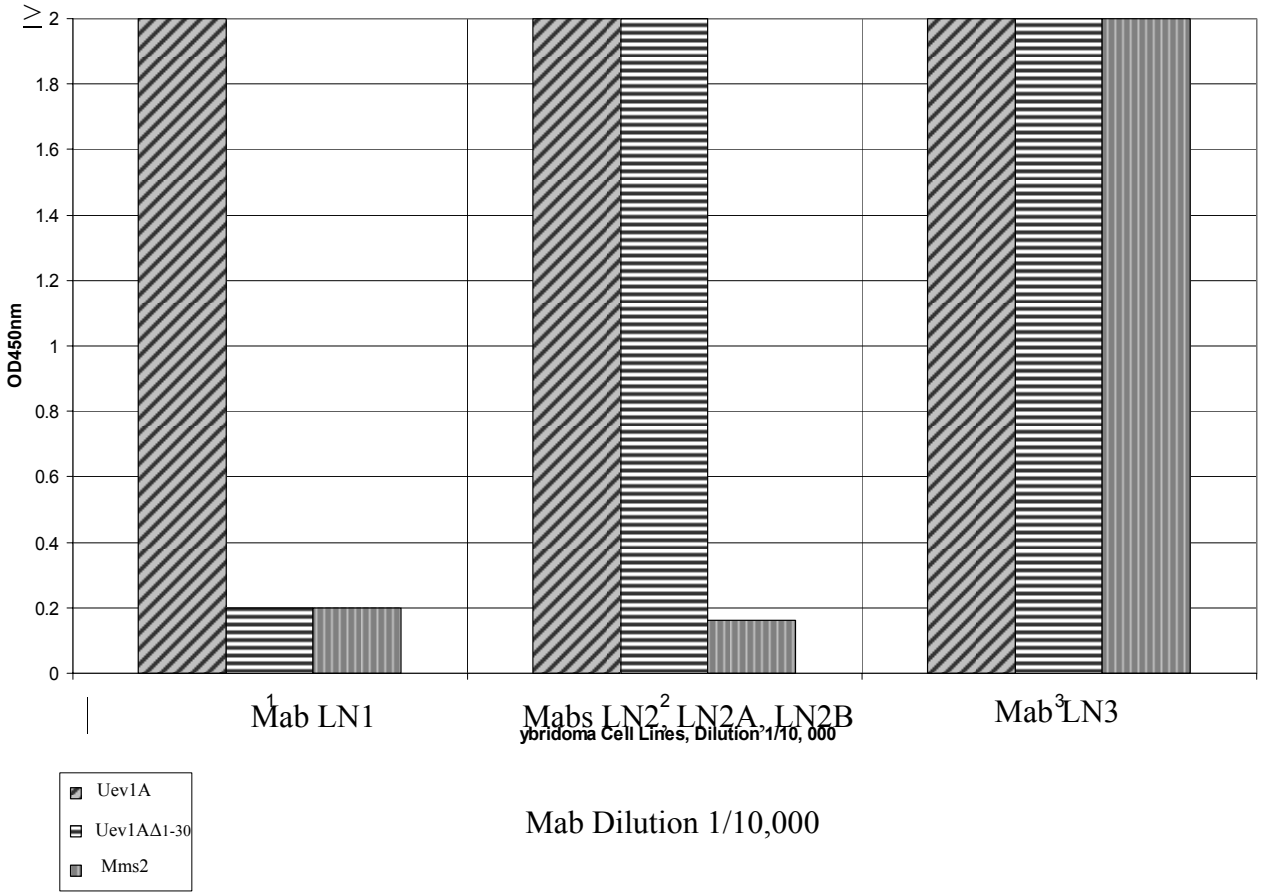

Figure 4-3. EIA at $OD_{450\ nm}$ for Mabs against Uev1A, Uev1AΔ1-30 and Mms2. Mabs LN1, LN2, LN2A, LN2B and LN3 binding specificity to Uev1A, Uev1AΔ30 and Mms2 as determined by the absorbance at $OD_{450\ nm.}$ Mabs in the form of ascites fluid were used.

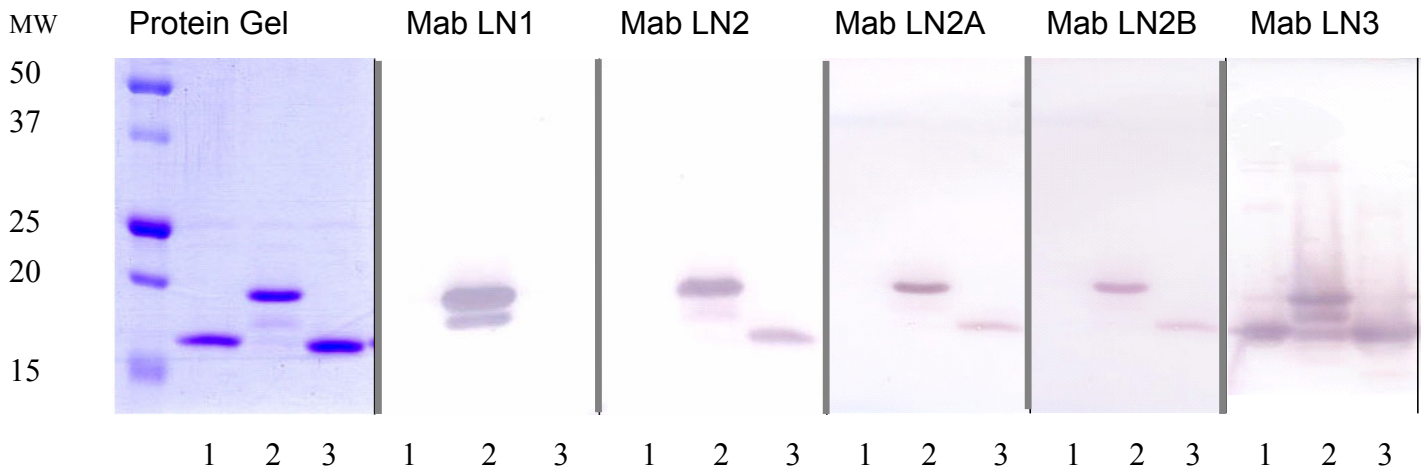

Antigen

1 – Mms2
2 – Uev1A
3 – Uev1AΔ1-30

Figure 4-4. Western blot analysis of Mabs LN1, LN2, LN2A, LN2B and LN3. Proteins Uev1A, Uev1AΔ1-30 and Mms2 were transferred to a PVDF membrane and Mab ascites fluid, at a dilution of 1/2,000, was used as the primary antibody.

A.

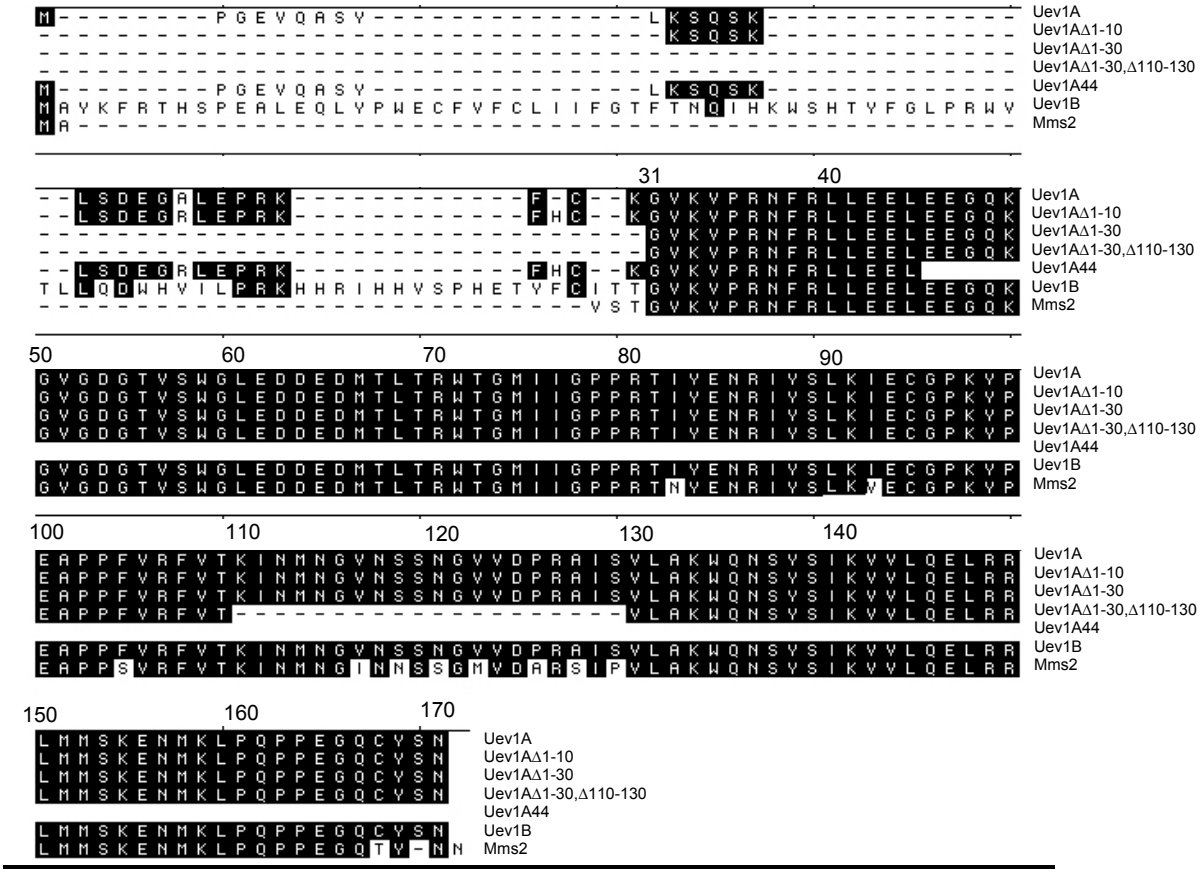

B.

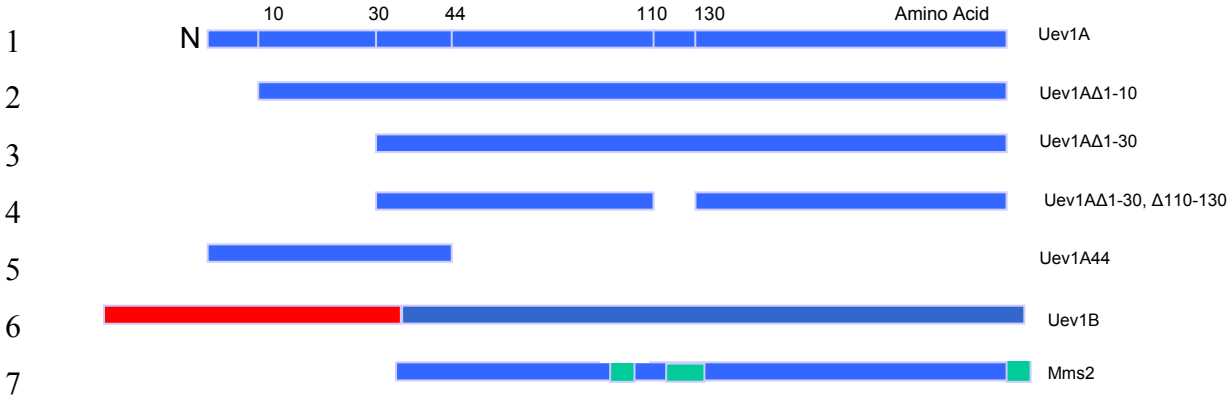

Figure 4-5. A. Amino acid sequence comparison of human Ubc variants Uev1B, Mms2, Uev1A and Uev1A-deletion constructs. Numbering is based on Uev1A a.a. sequence beginning at a.a. 31. **B. Pictorial representation of Uev1A-deletion constructs.** Green and orange colors designate amino acids in Mms2 and Uev1B, respectively, which are not the same as Uev1A.

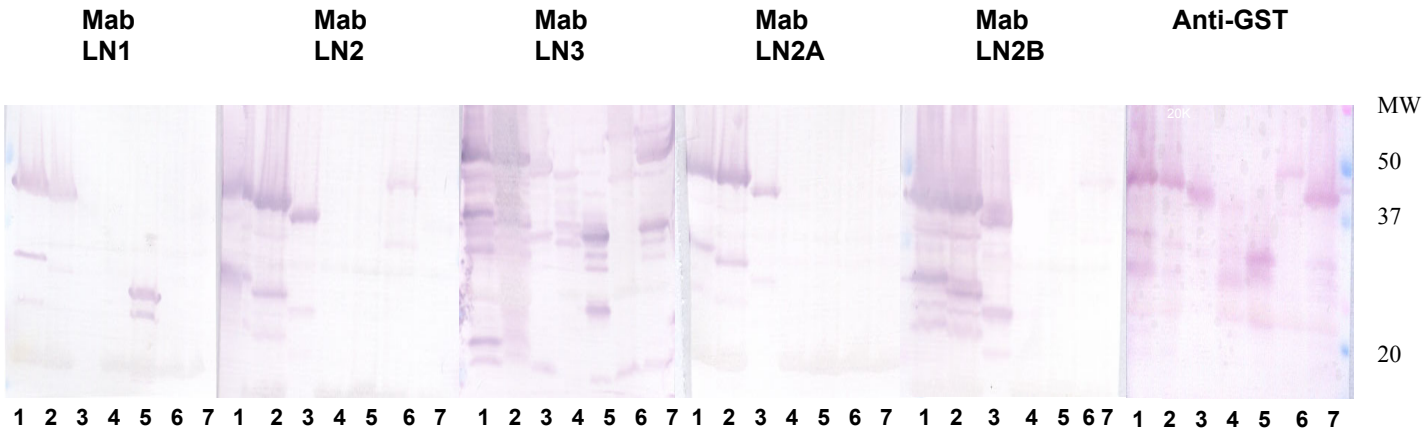

Legend

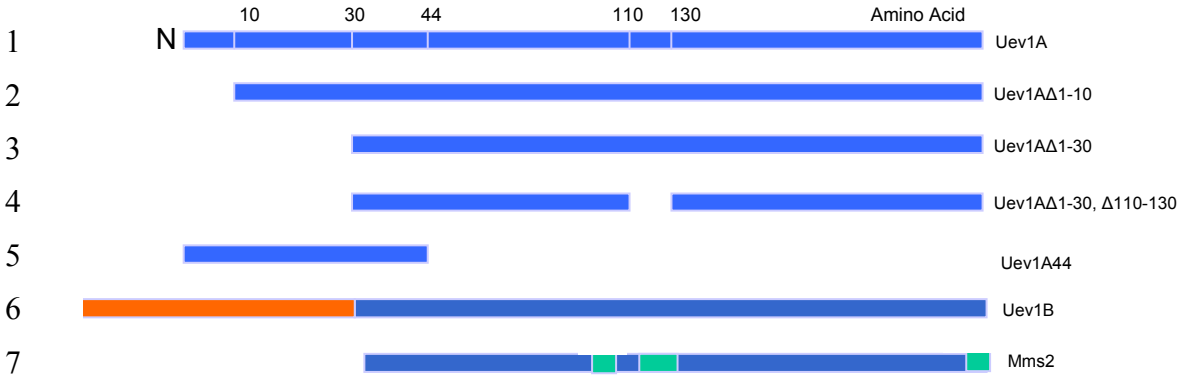

Figure 4-6. Western blotting analysis showing specificity of Mabs to Uev1A. Binding specificity of Mabs, was determined using five Uev1A-deletion constructs, Mms2 and Uev1B in Western blotting. Green and orange colors designate amino acids in Mms2 and Uev1B, respectively, which are not the same as Uev1A.

Mab LN1 only shows a binding response to Uev1A, Uev1AΔ1-10 and Uev1A44 in Western blot analysis. This result provides evidence that when a.a. 10-30 are missing Mab LN1 will not bind the protein and when they are present binding is observed. Mabs LN2, LN2A and LN2B show similar binding phenotypes to one another. All three Mabs bind to Uev1A, Uev1AΔ1-10, Uev1AΔ1-30 and Uev1B. This provides evidence of binding to the Uev1A unique core region as the other constructs are missing a.a. 110-130. Mab LN3 interacts with all constructs used in Figure 4-6, even Uev1A44. Its binding specificity can be deduced as a result of Mab LN3's ability to bind to Uev1A, Mms2 and also Uev1A44. As Mab LN3 does bind to Uev1AΔ1-30, it must be interacting within a.a. 30-44 of Uev1A.

4.5 Competition analysis and epitope mapping of Mabs

In addition to characterizing specific sequence targets of each Mab, the question arose of how many epitopes Mabs LN2, LN2A and LN2B bound to in the unique core region of Uev1A. In order to answer this question, each Mab's ability to compete with every other Mab was tested. In order to perform competition analysis, Mabs LN1, LN2, LN2A, LN2B and LN3 were each conjugated to HRP. Essentially, epitope mapping investigated the ability of each Mab to compete with the HRP-conjugated homologous Mab and all other HRP-Mabs to bind Uev1A in EIAs. For example, Mab LN1-HRP was allowed to bind Uev1A following binding of Mab LN1, LN2, LN2A, LN2B or LN3 binding to Uev1A. Enzyme substrate was allowed to develop and only if Mab LN1-HRP was able to bind would color development be observed. The relative competition index is calculated as explained in Section 3.6.2.2. Firstly, the reciprocal dilution from the direct binding assay at $OD_{450\ nm}$ = 1.0 is defined as 100% binding and this is compared to the ability of the Mab-HRP to compete at 50%. This was called the competition index.

This value was then divided by the homologous Mab competition index. Therefore, these calculations define the ability of one Mab to compete with another given Mab-HRP by directly comparing it to the ability of that particular Mab to compete with its own (i.e, the homologous) Mab-HRP. Using this theory and methodology it has been concluded, as seen in Table 4-3, that Mab LN1 competes with Mab LN3 and Mab LN2 competes with Mab LN2B. Additionally, Mab LN1 competes Mab LN3 better than Mab LN3 can compete Mab LN1.

Illustrations of Uev1A structure and Mab binding competition are shown in Figures 4-7 and 4-8. Fundamentally, because Mabs LN1 and LN3 are spatially adjacent, it is possible that they could inhibit binding of each other to variable extents. Mabs LN2 and LN2B are proposed to both bind the same sequence within the core 110-130 a.a. of Uev1A and, Mab LN2A is also defined to bind to that region. However, binding of Mab LN2A-HRP is not inhibited by Mabs LN2 or LN2B nor are Mabs LN2-HRP or LN2B-HRP inhibited by binding of Mab LN2A. Mab 2H11 is a Uev1A- and Mms2-binding Mab produced by Parker Andersen which does not appear to inhibit the binding of any other Mab, including Mab LN3, which also binds to both Uev1A and Mms2.

4.6 Epitopes in the core region of Uev1A

Following extensive study of the core structure of Uev1A, using NMR solution structure data, three putative antibody epitopes have been revealed. As can be observed in Figure 4-9, the unique Phe104, the unique sequence VNSSN at a.a. 115-119 and the unique sequence PRAISV at a.a. 125-130 may form three unique core epitopes. The possibility that there are three binding epitopes within the core region supports the notion that sequence differences between Uev1A and Mms2 may be critical to their functional

Table 4-3. Relative competition index of Mabs.

	Competing Mab					
Mab:HRP	**Mab LN1**	**Mab LN2**	**Mab LN2A**	**Mab LN2B**	**Mab LN3**	**Mab 2H11**
Mab LN1-HRP	1	>50	>50	>50	**6.5**	>50
Mab LN2-HRP	>50	1	>50	**0.5**	>50	>50
Mab LN2A-HRP	>50	>50	1	>50	>50	>50
Mab LN2B-HRP	>50	**2.1**	>50	1	>50	>50
Mab LN3-HRP	**0.9**	>50	>50	>50	1	>50

Bolded numbers are to emphasize the competition between Mabs LN1/LN3, and Mabs LN2/LN2B for binding to Uev1A. A value of >50 indicates the two Mabs do not inhibit each other's binding.

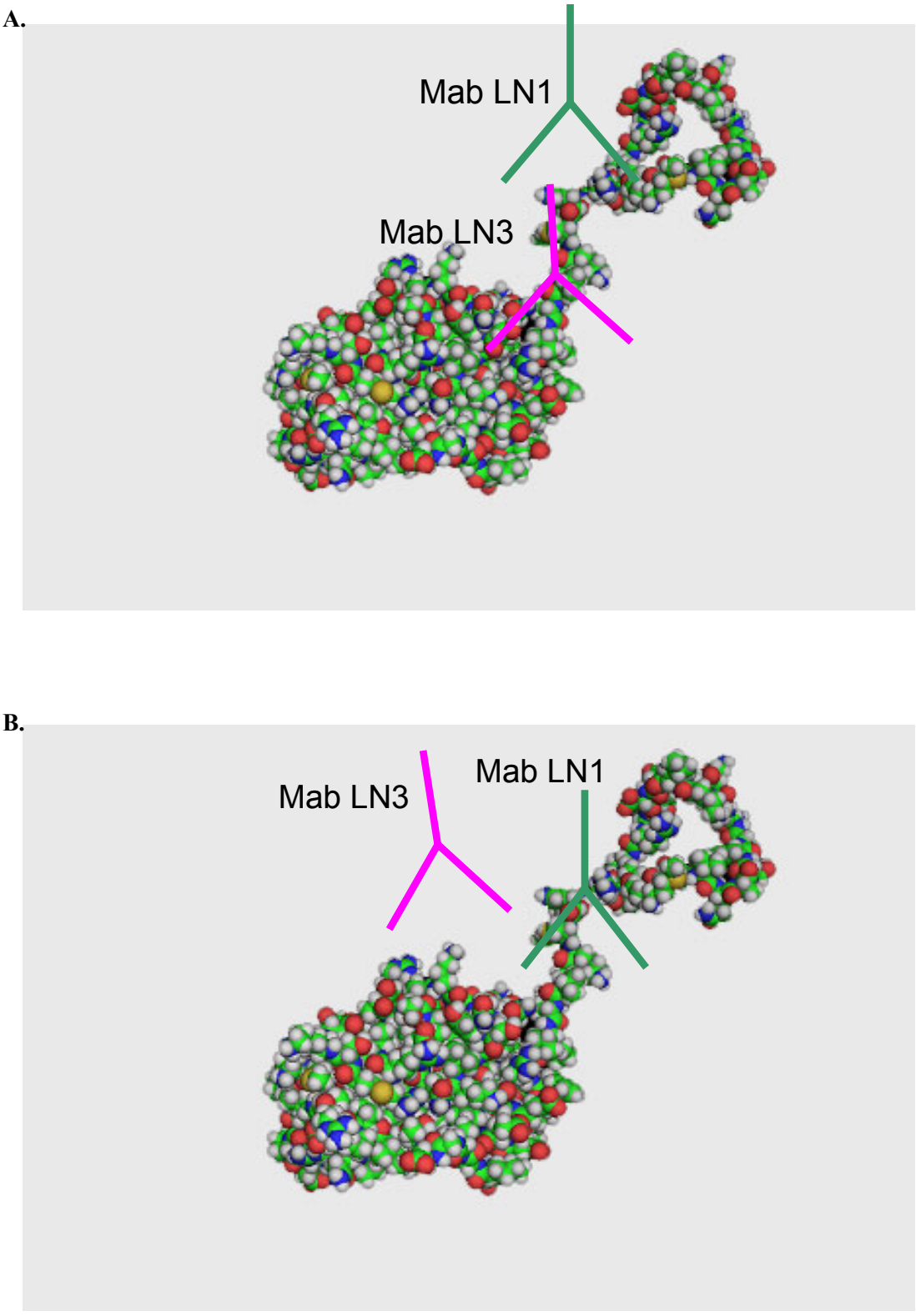

Figure 4-7. Putative binding competition for Mabs LN1 and LN3. Mabs LN1 and LN3 inhibit one another from binding to their distinct epitopes. **A**. Mab LN1 binds to the unique 10-30 a.a region of Uev1A. **B.** Mab LN3 binds to the Mms2 common 30-44 a.a region of Uev1A. These sequences are spatially adjacent.

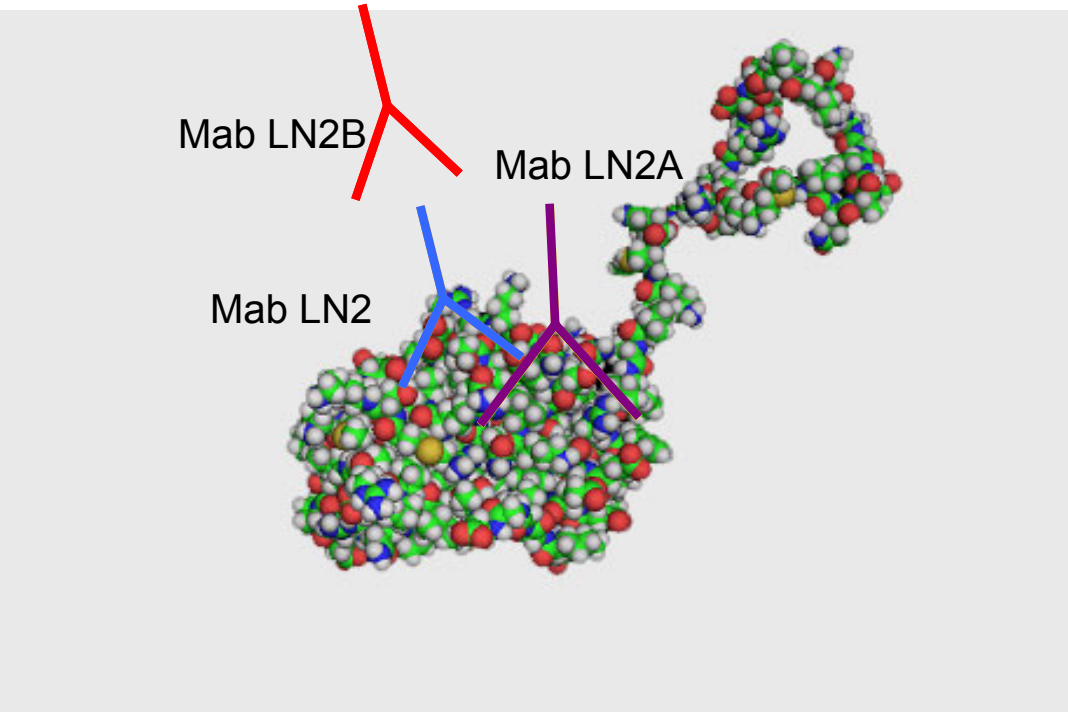

Figure 4-8. **Putative binding competition for Uev1A unique core specific Mabs LN2, LN2A and LN2B.** Mabs LN2 and LN2B inhibit one another from binding to the same epitope, but neither inhibits Mab LN2A. All three Mabs bind within the a.a. 110-130, where seven of fourteen a.a. are variable between Uev1A and Mms2.

differences within cellular signaling pathways. The three-dimensional structure in Figure 4-9 shows how Phe104 may be part of an epitope which is distinct from the VNSSN at a.a. 115-119 or it may be part of the same epitope due to its adjacent location in the folded protein. These three putative epitopes in the core region are found opposite to the Ub binding site and independent of the Ubc13 binding site. The side chains of Uev1A-Ile57 and Ub-Ile44 are required for Ub binding to the acceptor site of the Uev1A-Ubc13 complex for chain assembly *in vitro*. Uev1A-Asn37 and Uev1A-Phe38 have been shown to be required for binding to Ubc13 (Pastushok et al., 2005). Consequently, defining the three Mabs (LN2, LN2A and LN2B) to the unique core region of Uev1A and one Mab (LN1) to the N-terminal unique region of Uev1A could be of great potential to research, diagnostics and therapeutics in cancers stimulated by Uev1A/NF-κB.

4.7 Uev1A core mutations: Mab reactivity to a.a. mutations in variable core

Three mutants of *UEV1A* were cloned into pGEX-6P. These *UEV1A* mutants contained a.a. substitutions changing them from the Uev1A to the Mms2 sequence within the variable core region. Firstly, a Uev1AΔ1-30 construct was created containing an Phe–to-Ser mutation at a.a. 104. This construct was named Uev1AΔ1-30F104S. Secondly, a Uev1AΔ1-30 construct containing a five amino-acid substitution from a.a. 115-119 of Uev1A was constructed. The a.a. were changed from the Uev1A sequence VNSSN to the Mms2 sequence INNSS. This construct was named Uev1AΔ1-30+5. Finally, Uev1AΔ1-30 construct containing six a.a. substitutions from a.a. 125-130 of Uev1A was constructed. The a.a. were changed from the Uev1A sequence PRAISV to the Mms2 sequence ARSIPV. This contruct was named Uev1AΔ1-30+6. These proteins were all fused to GST when overexpressed in *E. coli* RIL cells. Crude protein extracts

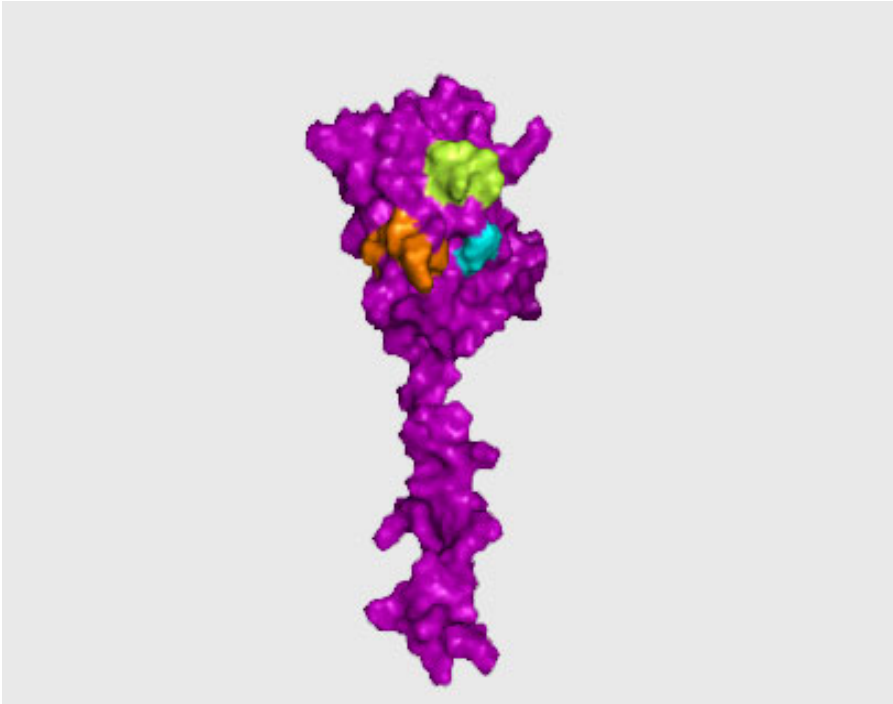

Figure 4-9. Three putative core epitopes in Uev1A. Uev1A is seen here in purple. Blue color highlights the Uev1A unique a.a. Phe104. Green color highlights the Uev1A unique sequence VNSSN at a.a. 115-119. Orange color highlights the Uev1A unique sequence PRAISV at a.a.125-130.

were used in Western blot analysis against the five Mabs. Figure 4-10 contains all Mms2 and Uev1A full length and deletion contructs, including those shown in Figure 4-6. Figure 4-10 shows the Mab specificity for the three core Uev1Amutants. Mab LN1 has been characterized to bind only to the N-terminal region of Uev1A within a.a. 10-30. Mab LN1 was not expected to have reactivity to any of the three core mutated Uev1A proteins and those expectations were proven correct. Mabs LN2, LN2A and LN2B were of most interest when testing these constructs. Following previous attempts to characterize these three core-specific Mabs, definative results characterizing the exact region of binding to Uev1A were not attained. Figure 4-10 provides further verification that Mabs LN2 and LN2B do possess the same binding pattern to GST-Uev1AΔ1-30F104S and GST-Uev1AΔ1-30+5. These Mabs were found to compete with one another for binding to Uev1A in epitope mapping experiments as seen by their relative competition indicies in Table 4-3. Furthermore, Mab LN2A is also a core binding Mab as is shown in Figure 4-6. Mab LN2A does not compete with Mabs LN2 or LN2B for binding to Uev1A as shown in Table 4-3. Additional proof of this Mab's differential binding to the core is shown (Figure 4-10) in its absence of reactivity to GST-Uev1AΔ1-30F104S and GST-Uev1AΔ1-30+5. The lack of reactivity to GST-Uev1AΔ1-30+6, in Figure 4-10, is explained by a lack of overexpression. Therefore, it is assumed that this protein was not present on the Western Blot and, therefore, there is a lack of reactivity.

4.8 Mab binding to Uev1B

Mabs LN1, LN2, LN2A, LN2B and LN3 were assayed for their binding phenotype to the Uev1B protein. As mentioned before, Uev1B is a splicing variant of *UEV1* that has the identical Uev domain like Uev1A, but contains distinct N-terminal

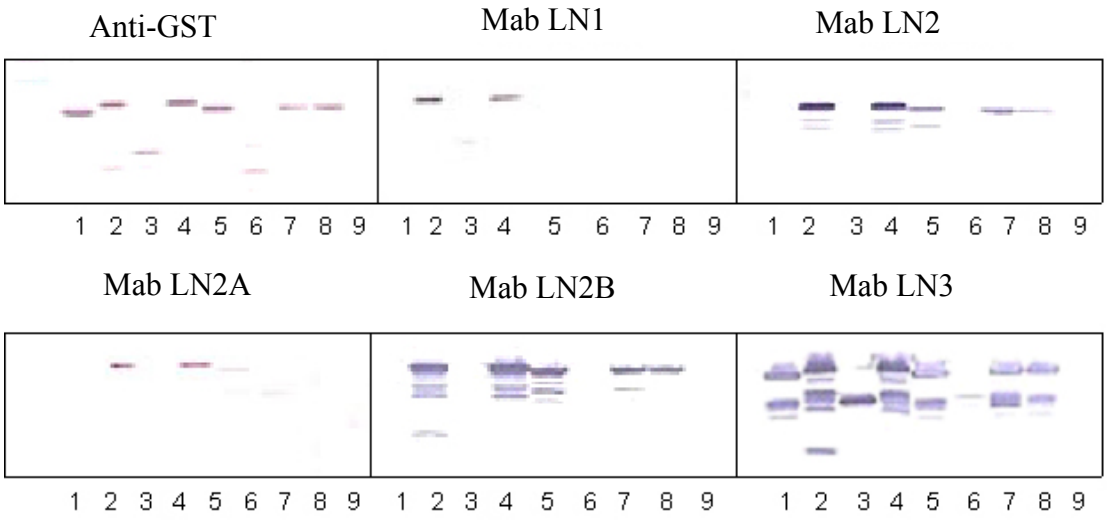

Antigen

1 GST-Mms2
2 GST-Uev1A
3 GST-Uev1A44
4 GST-Uev1AΔ1-10
5 GST-Uev1AΔ1-30
6 GST-Uev1AΔ1-30, Δ110-130
7 GST-Uev1AΔ1-30F104S
8 GST-Uev1AΔ1-30+5
9 GST-Uev1AΔ1-30+6

Figure 4-10. Western blot analysis of each Mab with Uev1A-deletion and mutant constructs. Uev1A-deletion and mutant contructs are used to analyze the binding specificity of the Uev1A unique core-specific Mabs LN2, LN2A and LN2B. All six Western blots showed no primary antibody binding to GST-Uev1AΔ1-30+6 as can be explained by a lack of overexpression.

sequences (Figure 4-5A). The cellular function of Uev1B is not currently known. Although, it is known that Uev1B does not physically interact with Ubc13 (Andersen et al., 2005) and is excluded from the nucleus (P.L. Andersen, unpublished data). Figure 4-11 shows Mab reactivity of the GST antibody, Mab LN2 and Mab LN3 with GST-Uev1B as was expected. Binding sequences previously determined for Mabs LN2 and LN3 are identical between Uev1A and Uev1B. Mab LN1 does not show reactivity to GST-Uev1B as is expected due to its specificity to the N-terminal region of Uev1A.

4.9 Mab LN1 binding to Uev1A in formalin-fixed paraffin-embedded tissue

Mab LN1 is the only Mab which has been successfully used for Uev1A staining in formalin-fixed paraffin-embedded tissue samples. Mabs LN2, LN2A, LN2B and LN3 did not successfully stain in all tissues tested. These results were obtained with the help of Dr. Emina Torlakovic of the Department of Pathology and Laboratory Medicine in the College of Medicine at the University of Saskatchewan. Figure 4-12 illustrates cytoplasmic and nuclear Mab LN1 staining of Uev1A in normal thyroid cells. Results show a loss of antibody binding when Mab LN1 is preabsorbed with the Uev1A purified protein. Figure 4-13 shows Mab LN1 reactivity with Uev1A in gastrointestinal cancer tissues. These tissue sections contain normal cells adjacent to the cancer cells, as indicated by the dashed line. Four of twenty adenocarcinomas of the gastrointestinal tract tested using immunohistochemistry were shown to have cytoplasmic and nuclear staining of Uev1A. Due to the heterogeneity of cancer tissues, four of twenty adenocarcinomas found to be postitive for Uev1A is considered to be a significant number. *In situ* dysplastic/ mucosa with severe dysplasia, but no evidence of invasion, also showed overexpression in two of two cases, but to much lesser degree than in the invasive adenocarcinoma. These results have indicated

that it would be valuable to perform additional research on normal versus cancer tissues to screen for Uev1A expression.

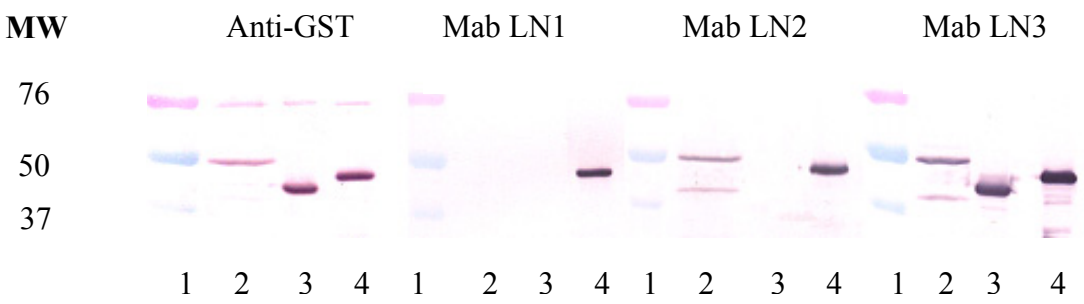

Legend:

1 marker
2 GST-Uev1B
3 GST-Mms2
4 GST-Uev1A

Figure 4-11. Mab binding to GST-Uev1B, GST-Mms2 and GST-Uev1A. Western blot analysis shows binding patterns of the three categories of Mabs isolated from the hybridoma screen to GST-Uev1B, GST-Mms2 and GST-Uev1A.

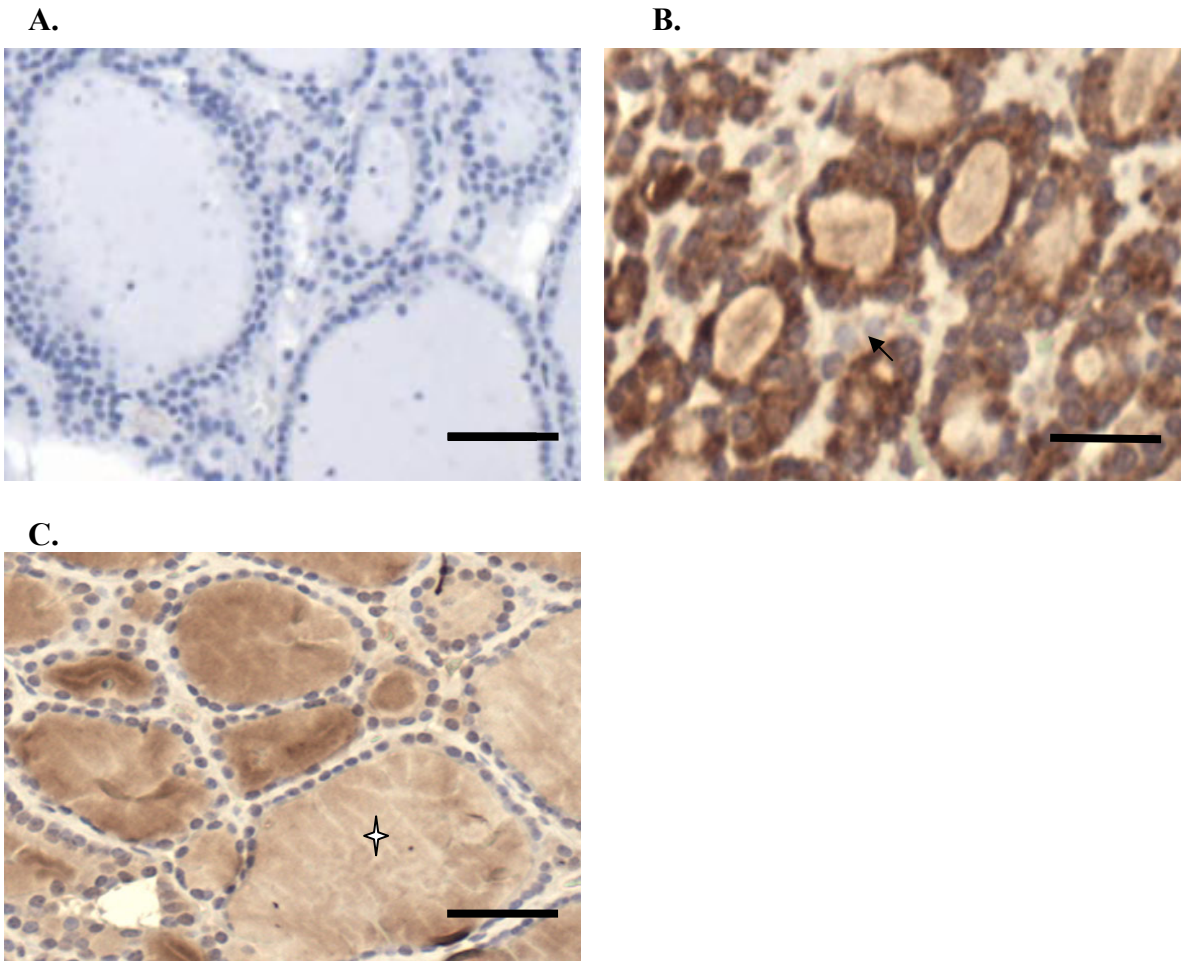

Figure 4-12. Mab LN1 binding specificity to Uev1A in normal thyroid formalin-fixed paraffin-embedded tissue. **A.** The negative control shows no staining in the cytoplasm or nuclei; the nuclei show blue color as a result of counterstaining with Haemotoxylin. **B.** Immunohistochemistry was performed with Mab LN1. Cytoplasmic staining was predominatly found. However, some variable staining of the nuclei was also observed. Note unstained cells in between the thyroid epithelium lining the follicles with thyrogolobulin, which support specific nature of the immunostaining by Uev1A Ab (arrows). Secreted thyroglobulin appears to show some weak non-specific staining (star). **C.** As an internal control, Mab LN1 was preadsorbed with Uev1A antigen which resulted in total loss of cytoplasmic and nuclear reactivity to Uev1A. Some non-specific staining of the secreted thyroglobulin remained (asterisk). The bar represents 50 μm.

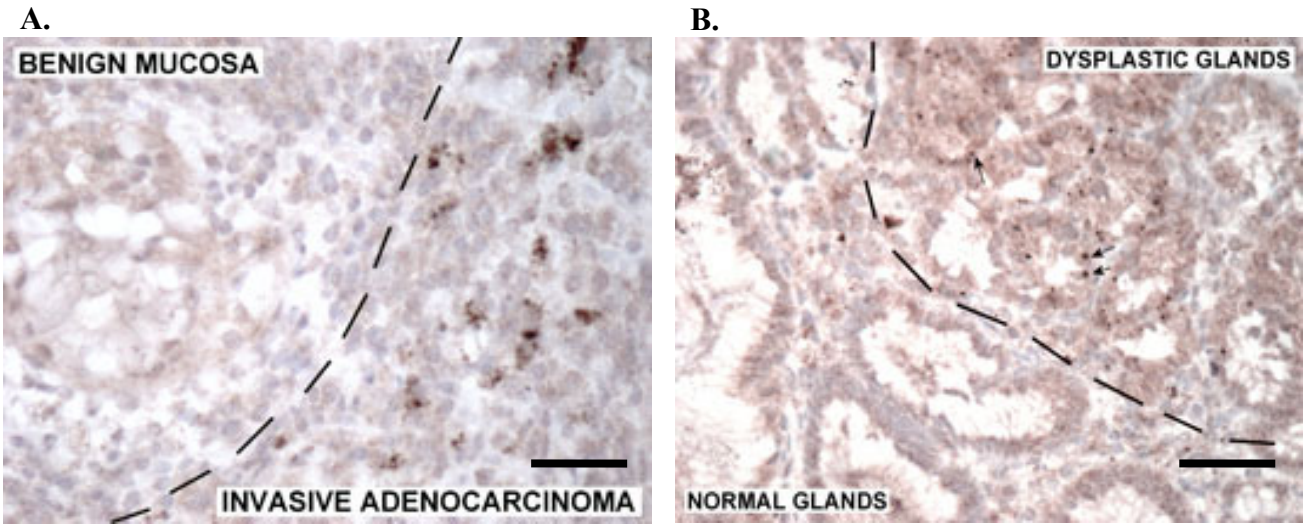

F**igure 4-13. Mab LN1 binding specificity to Uev1A in normal and formalin-fixed paraffin-embedded carcinoma tissue. A.** Invasive adenocarcinomas of the gastrointestinal tract showed cytoplasmic overexpression of Uev1A. Adjacent benign mucosa was present in this tissue sample and did not show Uev1A overexpression as indicated by the dashed line. **B.** Neoplastic mucosa with severe dysplasia/carcinoma *in situ* also showed overexpression of Uev1A, but the expression appeared much weaker than in the invasive adenocarcinoma. The bar represents 50 μm.

CHAPTER FIVE

DISCUSSION

5.1 Uev1A versus Mms2: sequence and structural implications for cellular function

The sequence and structural differences between the two Uevs, Uev1A and Mms2, must account for the distinct biological pathways by which they perform Lys63-linked polyubiquitination of cellular targets. Both Uevs function alongside Ubc13 to create these non-canonical ubiquitin chains. Obviously, the N-terminal Uev1A sequence of a.a. 1-30 differs from Mms2. However, the a.a. regions consisting of 104, 116-129 and 167-169, which also differentiate Uev1A and Mms2, cannot be overlooked. In fact, any of these regions of Uev1A may contribute to Uev1A's differential cellular signaling function. Epitopes may be as small as eight a.a. (Dreyer and Bennett, 1965). Therefore, multiple epitopes may exist within the N-terminal region for which one Mab has been defined (LN1). Additionally, examination of the core structure of Uev1A has revealed that F104 is situated adjacent to the seven variable residues within a.a. 116-129 as shown in Figure 4-9. Three Mabs (LN2, LN2A and LN2B) have been characterized to bind the unique core of Uev1A within a.a. 110-130. Many overlapping epitopes may exist in this unique region. However, Mabs LN2 and LN2B are expected to bind the same epitope, based on results from EIA competition and Western blotting, and Mab LN2A is expected to bind to a different epitope than both Mabs LN2 and LN2B. Essentially, three Mabs have been found to bind to at least two epitopes within the unique core region of Uev1A.

The differences in a.a. sequence must be important for distinguishing Uev1A and Mms2 function. Due to the old age of the BALC/c female mice used for Uev1A

immunization and subsequent hybridoma fusions, it was expected to obtain antibodies to any region of the Uev1A protein. See section 2.6 for further explanation in this regard. The C-terminal a.a. 167-169 differ from Uev1A to Mms2. This is a region of the Uev1A that is located on the exteriorof the protein structure. It is therefore expected that an antibody could have been generated to this region but, it was not obtained. One of the three Uev1AΔ1-30 binding Mabs lost in the hyrbridoma screen may have bound to the Uev1A C-terminal region. However, it is also possible that the inbred BALB/c mice used for immunization were not capable of producing antibodies that would be specific to this putative epitope because they did not contain the genes necessary to do so.

The difference in the sequences of Uev1A and Mms2 are possibly important for interaction with an inhibitor or activator, or may be subject to covalent modification in order to alter the activity of Uev1A. Additionally, another possible functional difference may arise for Uev1A if it performs auto-cleavage of its N-terminus for signaling or functional purposes. Previously demonstrated experimental truncation of the N-terminus of Uev1A (Andersen et al., 2005) caused Uev1A localization to change within the cell when compared to full length Uev1A. In fact, Uev1AΔ1-30 and Mms2 were both shown to be localized to the nucleus following DNA damage treatment, whereas Uev1A was not (Andersen et al., 2005).

5.2 Success in selecting Uev1A-specific Mabs

Many factors may have attributed to finally obtaining the Mabs of the desired Uev1A-specificity. The timeline for immunizing BALB/c female mice, illustrated in Figure 3-3, may have played an important role in providing hyribdoma clones capable of binding the unique epitopes of Uev1A. The mice used for hybridoma fusions were immunized five times. Each mouse was administered 35 μg on the first immunization

and subsequently boosted four times with 17.5 μg. These immunizations were administered over the period of one year prior to performing hybridoma fusions. Firstly, it is believed that within this immunization timeline, antibodies of higher affinity and avidity would have been produced due to V(D)J recombination and hypermutation as discussed in Section 2-3. Each immunization would provide B cells the opportunity to produce antibodies with increased affinity and avidity for the antigenic epitopes. Additionally, upon repeat immunizations there is a higher probability of obtaining antibodies of the IgG versus the IgM class (Uhr and Moller, 1968).

5.3 Mab LN1: an N-terminal Uev1A-binding Mab

Following selection of four Mabs capable of distinguishing Uev1A from Mms2, each Mab's epitope specificity was assesed. Mab LN1 was not the only initial putative N-terminal specific Mab. Indeed, six putative Mabs capable of binding to Uev1A, but not Uev1AΔ1-30 or Mms2 had been isolated. However, through the screening process some Mabs either lost reactivity or were dropped from the screen due to being an IgM class. Subsequently, Mab LN1 was the only N-terminal Uev1A-specific Mab successfully recloned and characterized. Analysis of the binding pattern of Mab LN1 in both EIA and Western blotting was employed following the molecular cloning of deletion and a.a. substitution mutants of Uev1A. Mab LN1 was found to bind Uev1A within a.a. 10-30.

Mab LN1 competition with Mab LN3 could prove to be a significant and valuable discovery. Mab LN3 was found to be specific to the epitope containing a.a. 30-44 of Uev1A. Consequently, Mab LN3 binds to the location near Asn37 and Phe38 residues which are necessary for Ubc13 binding to Uev1A. Could Mab LN3 be employed to inhibit Ubc13 binding to Uev1A? It is probable that an antibody may inhibit binding of

another protein. However, the sequence from a.a. 30-44 of Uev1A is precisely the same as Mms2 and therefore Mab LN3 could not be used to differentiate Uev1A from Mms2 for the purpose of inhibition. Inhibiting the function of Mms2 could cause the demise of a cell's genome stability. For that reason, Mab LN3 cannot be used to specifically inhibt Uev1A-Ubc13. However, Mab LN1 is capable of blocking Mab LN3 from binding to Uev1A. Thus, it may also be capable of blocking Ubc13 from binding Uev1A. Indeed, without Ubc13 binding, Uev1A is unable to promote Lys63-linked polyubiquitin chains and NF-κB signaling could be abolished.

Competition analysis showed Mabs LN1 and LN3 to compete for binding to Uev1A. Due to their different sequence specificity in Western blot analysis (Figure 4-6), Mabs LN1 and LN3 must not compete for the same binding site, but rather block each other from binding to Uev1A at adjacent sites. IgG antibodies have a MW of 150,000 and HRP has a MW of 40,000. HRP-IgG conjugation reactions are expected to yield three-four HRP molecules bound to one IgG molecule when allowed to bind at a mole/mole ratio. A molecule the size of HRP-IgG could be from MW 270,000 to 310,000. Therefore, IgG at a MW of 150,000 may efficiently block binding of an HRP-conjugated Mab at a MW of 270,000 to 310,000 to the same or adjacent binding sites on a protein with the folded structure of Uev1A, at a MW of 18,700. The three-dimentional solution structure of Uev1A obtained through nuclear magnetic resonance technology has been presented in this thesis. This structure permits investigation of the topography of the folded Uev1A protein. Based on the Uev1A structure and the relative competition index values attained, it is clear that Mab LN1 binds an epitope of Uev1A which is more topographically accessible than the epitope for Mab LN3, as illustrated in Figure 5-1.

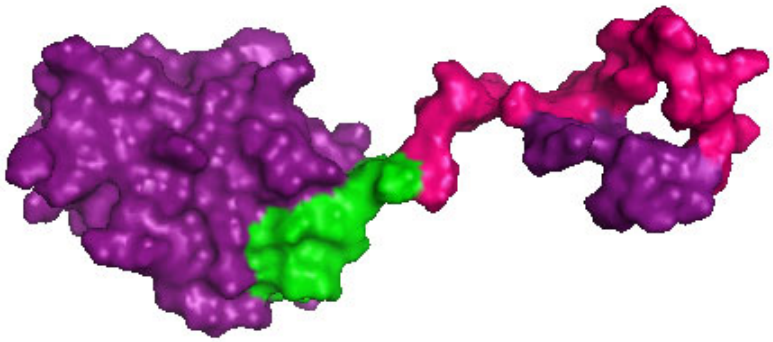

Figure 5-1. Surface topography of Uev1A and putative binding epitopes of Mabs. Uev1A Mab LN1 is specific for the region of Uev1A from a.a. 10-30 designated in pink. Mab LN3 is specific for the region of Uev1A from a.a. 30-44 designated in green. As can be observed from this image, Mab LN1 is able to bind to a more topographically accessible region of the protein and block the binding of Mab LN3 to a less accessible site.

Mab LN1 was the only Mab successfully used in immunohistochemistry staining of formalin-fixed paraffin embedded tissues. Binding of Mab LN1 was observed in the cytoplasm and nucleus of normal thyroid tissue. Interestingly, the core-specific Mabs LN2, LN2A and LN2B did not show any binding in these experiments. Previous experimentation has shown some Mabs are not useful for staining in fixed-tissue immunohistochemistry, while the same Mabs may be of use for staining fresh tissue sections (Torlakovic. E., personal communication). The reasoning for this is unknown. Nevertheless, Mabs LN2, LN2A and LN2B may be useful for fresh tissue staining. Another possibility for the lack of staining by Mabs LN2, LN2A and LN2B is that the unique core of Uev1A may be blocked by a covalent modification or protein binding to this region. This would result in a condition whereby Mabs LN2, LN2A and LN2B could not bind to Uev1A *in situ*.

Assessment of Uev1A in SDS-PAGE shows two smaller MW bands (Figure 4-1). These lower MW bands may be naturally cleaved or truncated Uev1A molecules. These bands were noted in the early stages of this Master's research. However, these low molecular weight protein bands were not sequenced due to the discovery of differential binding to these proteins by the Mabs obtained. Mab LN1 appears to bind only to Uev1A and the middle MW band, whereas Mabs LN2, LN2A, LN2B and LN3 bind to all three protein bands. The two smaller protein bands are expected to be approximately 155 and 140 a.a based on migration in SDS-polyacrylamide gels. As a result, it is presumed that there may be autocleavage of the Uev1A protein from the N-terminus. The Mab LN1 binding specificity to only the larger two protein bands provides supporting evidence for this as can be observed in Figure 4-4. Furthermore, it should be noted here that the crystal structure of full length Uev1A could not be resolved. Only when the N-terminal sequence was removed and a Uev1AΔ1-30 construct was used could the crystal structure

be resolved (Moraes. T., personal communication). Further investigation, using the formalin-fixed paraffin embedded tissues has only shown that Uev1A a.a 10-30 are present in these tissues. At this time, it cannot be proven or disproven, whether other natural truncations of Uev1A may exist *in vivo*. However, these observations may be of importance to further understand Uev1A functions.

5.4 Mabs LN2, LN2A and LN2B: Unique core Uev1A-binding Mabs

Mabs LN2, LN2A and LN2B were all found to be specific for the unique core region of Uev1A. Six Mabs of this desired specificity were isolated in the initial Mab screening process. Three were successfully recloned and characterized. Each core Uev1A-specific Mab was found to bind Uev1A, Uev1AΔ1-10, Uev1AΔ1-30, but not Uev1AΔ1-30,Δ110-130, Uev1A44 or Mms2 in EIA and Western blot. Assesment of the core was needed for further analysis of the binding specificities of Mabs LN2, LN2A and LN2B. Epitope mapping experiments revealed Mabs LN2 and LN2B to compete for the same or overlapping binding sites. Mab LN2A did not compete with either Mab LN2 or LN2B. Upon study of the NMR solution structure of the unique core region of Uev1A, three putative epitopes were defined as involving a.a 104, 115-119 and 125-130 as illustrated in Figure 4-9.

This information lead to the creation of three Uev1A mutants involving these a.a. sequences. By creating Uev1A protein constructs which contained core a.a substitutions, using the Mms2 sequence in place of the Uev1A sequence, it was expected that epitopes for each of the three Mabs could be ascertained by observing a loss of binding in Western blotting analysis. Therefore, three Uev1A mutants were created as outlined in Sections 3.1.1.3 and 4.6. These constructs were named Uev1AΔ1-30F104S, Uev1AΔ1-30+5 and Uev1AΔ1-30+6. Uev1AΔ1-30F104S contained a Phe-to-Ser mutation at a.a. 104,

Uev1AΔ1-30+5 contained replacement at a.a. 115-119 of Uev1A by the Mms2 sequence INNSS and Uev1AΔ1-30+6 contained replacement at a.a. 125-130 of Uev1A by the Mms2 sequence ARSIPV. These constructs containing limited Mms2 sequences were expected to maintain a similar folded structure as Uev1A so as to not disrupt Mab binding to any a.a. region still present. Also, these Mabs had previously been shown not to bind to these Mms2 a.a. sequences. These constructs helped to show that, indeed, Mabs LN2 and LN2B bind to an epitope distinct from the epitope recognized by Mab LN2A. Figure 4-10 shows Mabs LN2 and LN2B to bind Uev1AΔ1-30F104S and Uev1AΔ1-30+5, whereas Mab LN2A does not. This data illustrates that Mabs LN2 and LN2B may bind to Uev1A a.a. 125-130 as they still bind to those proteins which contain this sequence, but have mutations in the other unique core sequences. At this time, it cannot be proven that Mab LN2A binds to a.a. 115-119 as the protein Uev1AΔ1-30+6 was not blotted successfully due to a lack of expression. However, Mab LN2A did not bind to Uev1AΔ1-30F104S or Uev1AΔ1-30+5 which does provide evidence of a differential binding pattern from Mabs LN2 and LN2B.

Additionally, the Uev1AΔ1-30 a.a. region from 125-130 was mutated at arginine 126 to an alanine and overexpressed. This R126A mutation was made because this arginine was found to be the most topographically accessible within the region from a.a. 125-130. However, following Western blotting analysis of this protein using Mabs LN1, LN2, LN2A, LN2B and LN3 it was found that all unique core binding Mabs bind Uev1AΔ1-30R126A. Therefore, Mabs LN2, LN2A and LN2B do not bind to an epitope dependent on arginine 126 of Uev1A (data not shown).

5.5 Future directions

In the immediate future, the Uev1A a.a. region from 124-130 should be mutated. Following investigation of the a.a. in this sequence, a Uev1AΔ1-30 construct containing substitutions at a.a. 124 and 128 from the Uev1A to the Mms2 sequence should be cloned. These a.a. affect the topography of adjacent arginine and lysine a.a. which Uev1A and Mms2 share in common. Subsequently, the differences in topography of the core epitopes are expected to depend on the a.a. at 124 and 128 of Uev1A. For example, Uev1A contains a serine at a.a. 128, whereas Mms2 contains a proline. Therefore, due to the molecular structure of these two a.a., the proline may cause an adjacent common a.a. to be situated at a different angle than the serine. Investigation of Uev1A lysine 132, which is common to Mms2, using the NMR solution structure, has shown that indeed this is the case. As illustrated in Figure 5-2, the arginine and lysine residues of Uev1A are the most topographically accesible a.a. adjacent to the core unique a.a at 124 and 128. Therefore, a Uev1A epitope containing a.a. 124-132 is expected to be important for binding of Mabs LN2 and LN2B. Western blotting analysis with Uev1AΔ1-30P124A,S130P is expected to provide the final answer as to what the Uev1A binding epitope is for Mab LN2A.

In order to validate the usefulness of these Mabs in biochemical and medical research, obtaining knowledge of some additional properties of Mabs LN1, LN2, LN2A and LN2B is necessary. In order to use the Uev1A-specific Mabs for diagnosis, the sensitivity for Uev1A binding in tissue staining must be researched to obtain titers for use in further experiments. Additionally, in order to understand any possible treatment potential for the Uev1A-specific Mabs, the ability to actually inhibit Uev1A function *in vivo* should be researched. This would require delivery of Mabs LN1, LN2, LN2A or LN2B into living cells in order to assay for a loss of Uev1A function. By asssaying the

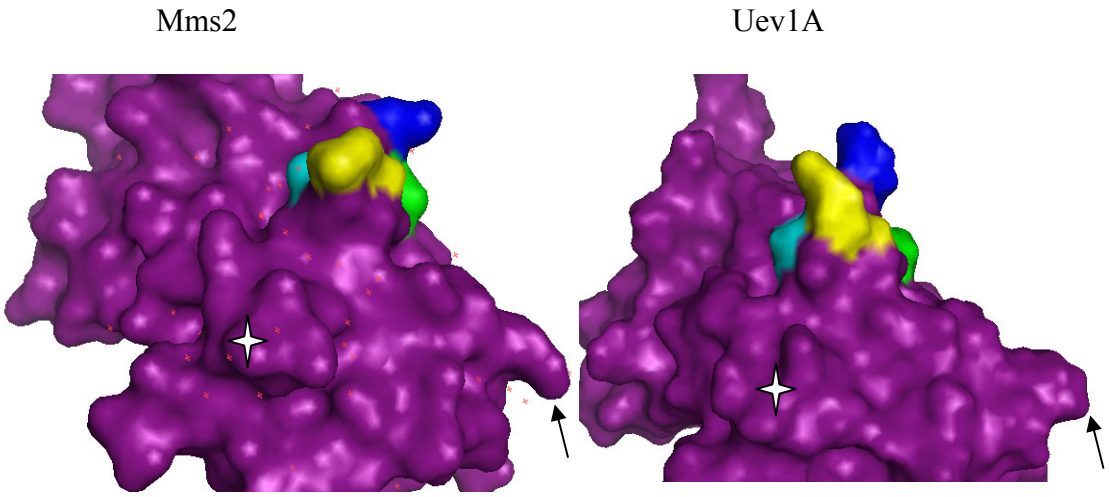

Figure 5-2. Comparison of the 3D structure of the core region of Uev1A from a.a. 124-132 to that of Mms2. NMR solution structure manipulations provide illustration and evidence of differential structure within the core a.a. from 124-132 of Uev1A when compared to corresponding a.a. in Mms2. Yellow designates Uev1A a.a. R124 and Mms2 a.a. R106. Blue designates Uev1A a.a. K132 and Mms2 a.a. K113. Green designates Uev1A a.a. S129 and Mms2 a.a. P109. Cyan designates Uev1A a.a. P125 and Mms2 a.a. A105. The white star and arrow are present for the purpose of orientation. The white star designates a.a. S100 of Mms2 and S119 of Uev1A. The arrow represents a.a. K134 of Mms2 and K154 of Uev1A.

ubiquitination status of NEMO or RIP1, blockage of function by Mabs LN1, LN2, LN2A or LN2B could be assessed. After attaining these primary short term goals, these Mabs could be used for further characterization of the Uev1A-Ubc13 heterodimer and its function within living cells. Additionally, further testing of cancer and noncancer tissues for overexpression of Uev1A may provide important insights for specific cancers. In fact, one overexpressed isoform of Uev1A could well be indicative of tumorigenesis. Mabs LN1, LN2, LN2A or LN2B may aid the discovery of this type of isoform-dependent Uev1A cancer signalling. As such, it may be possible to use these Mabs as a dignostic tool to detect a specific Uev1A isoform or for cancer treatment if an inhibitory Mab-drug could be developed and administered to patients. Additionally, small peptipdes containing the structure of an inhibitory Mab could be cloned following discovery of the Fab binding sequence and structure using mass spectrophotometry. These could be potentially used as a method of treatment for Uev1A-related cancers. Some possibilities are discussed in Section 5.8.

5.6 Applications and uses of Mabs

Milstein and Kohler won the Nobel prize in 1984 in physiology and medicine for their discovery of hybridoma technology because of its potential in laboratory experimentation, diagnostics and treatment. Mabs have become important for biochemistry, molecular biology and medicine. Mabs are used in research in many experiments that require localization of antigens both *in vitro* and *in vivo*. Mabs are useful for ascertaining biological functions of specific antigens through experimentation involving immunoprecipitations, Western blotting, enzyme immunoassays, immunofluorescence and immunohistochemistry. Mabs have also been used for diagnostics within the medical field. For example, commercial tests for pregnancy look

for the presence of the beta subunit of human chorionic gonadotropin in urine using a Mab present on the test surface. Additionally, medical laboratories can perform early diagnosis of the presence of pathogens involved in many diseases.

One limitation of the early work in this antibody field was that, although Mabs are capable of targeting specific cell structures, most are not potent enough on their own to induce cell death. Advances in technology to arm Mabs with cell-killing payloads have helped scientists overcome this constraint. Technologies have been developed leading to an increase in the potency of Mabs, whether the antibody internalizes or stays on the surface of the targeted cell (Wu and Senter, 2005). Subsequently, many Mabs have become useful for treatment of cancer and other diseases.

5.7 Antibody-based cancer therapy

To date, the federal drug administration has approved nine genetically engineered antibodies for the treatment of cancer. Rituxan is a chimeric anti-CD20 antibody and the first antibody approved for immunotherapy in non-Hodgkin's B-cell lymphoma. It is marketed by Genentech and Biogen IDEC (Plosker and Figgitt, 2003). Herceptin, also marketed by Genentech, is a Mab that targets the HER-2 protein on the surface of breast cancer cells (Albanell et al., 2003). Campath, marketed by Genzyme, targets the CD52 antigen and is used to treat patients suffering from B-cell chronic lymphocytic leukemia (Alinari et al., 2007). Erbitux, marketed by Imclone and Bristol-Myers Squibb for patients with colon cancer, is markedly specific for epidermal growth factor receptor (Wong, 2005). Vectibix, for patients with colorectal cancer, targets epidermal growth factor receptor. Bexxar and Zevalin are used for patients with non-Hodgkin's B-cell lymphoma and are specific for CD20. Avastin, marketed by Genentech for patients with

colon cancer, targets the vascular endothelial growth factor (Carter, 2001; Kramer and Lipp, 2007).

Antibody-drug conjugates (ADC) are an additional emerging therapeutic strategy for Mabs because they empower antibodies that have specificity for tumor cells, but no cell-killing capabilities. It is possible to deliver a potent, cytotoxic drug in a targeted manner to a tumor as compared to systemically injected drugs (Hamblett et al., 2004). Systemic administration of cytotoxic drugs is typically limited by toxicity resulting from exposure of normal tissues (Doronina et al., 2003). By utilizing an ADC, it may be possible to achieve a higher concentration of drug at the tumor while minimizing exposure to normal tissues. The federal drug administrataion approved the first ADC for cancer, Mylotarg®, in 2000. Mylotarg, marketed by Wyeth, links an antibody with the drug calicheamicin (Ricart and Tolcher, 2007), which is an enediyne class of antitumor antibiotic that binds to DNA and induces apoptosis. This treatment is used for patients with acute myeloid leukemia.

Therapeutic applications of Mabs are widespread. Although they have been used for some cancer therapies, not all cancers have been 'cured'. Cancer is genetically based disease. Many tumor suppressor genes may lose function and oncogenes may gain function with mutations caused by carcinogens, resulting in tumorigenesis. Some cancers have treatments available, but many do not. Mabs have proved to be a useful tool and in years to come there may be many more federal drug administration-approved Mab-based drugs.

5.8 Research, diagnostic and treatment potential for Uev1A-specific Mabs

The research potential of these Mabs may be widespread based on their usefulness in many experiments as previously mentioned in Section 5.6. It is interesting to note that

Mabs specific for Ubc13 and Uev1A/Mms2 have been raised in Dr. Wei Xiao's research laboratory. These Mabs have been licenced to Invitrogen and Santa Cruz by the University of Saskatchewan. Mabs LN1, LN2, LN2A and LN2B should be considered even more valuable as they differentiate between Uev1A and Mms2. Therefore, there is expected to be considerable research potential for Mabs LN1, LN2, LN2A and LN2B.

The treatment potential of each of Mabs LN1, LN2, LN2A and LN2B is unknown at present. Firstly, the Mab must have the ability to specifically recognize Uev1A. The results presented here prove this goal has been reached. Secondly, the Mab would need to be humanized, or made into a chimera to prevent the Human Anti-Mouse Antibody (HAMA) response. Initial clinical studies found Mabs to be of limited therapeutic value, because early mouse-derived Mabs often resulted in an immune system response by patients. When injected into humans, a mouse Mab is usually recognized by the body's immune system as being foreign. The human immune system therefore responds by rapidly neutralizing the mouse Mab and rendering it ineffective for further therapy, a reaction referred to as a HAMA response (Thorpe et al., 2003). Over the past three decades, researchers have developed a number of approaches to make mouse Mabs appear more human-like to a patient's immune system, thereby lowering the risk of inducing an immune response. These technologies have enabled scientists to develop antibody products that can be administered to patients repeatedly over time with reduced adverse responses by the human immune system. A therapeutic Mab can be chimeric, humanized or fully human (Neuberger et al., 1985). A chimeric Mab contains a mixture of both mouse and human sequences, usually a 30/70 split, respectively, where the mouse components are responsible for binding to the antigen and the human components are involved in inducing a therapeutic effect. Humanized Mabs contain over 90 percent

human sequences, while fully-human Mabs contain 100 percent human sequences (O'Kennedy and Roben, 1991).

Thirdly, the Mab would need to have a drug conjugated that would induce apoptosis of target cancer cells. As mentioned above, calicheamicin can be used as a potent cell-killing agent. How would a Mab be linked to calicheamicin and specifically target cancer cells if the overexpressed cancer causing antigen is inside the cell? Calicheamicin is a potent cytotoxic agent that causes double-strand DNA breaks, resulting in cell death. If this chemical was linked to any of the Mabs reported in this thesis, many issues may arise. For example, a calicheamicin-linked Mab LN1, LN2, LN2A or LN2B would not be able to recognize the exterior of the cancer cells, and acquire access to the inside of the cell. But it would be necessary to target cancer cells on the exterior before any killing action is taken as Uev1A is found in all eukaryotic cells. This would be crucial to reducing total cell killing. Therefore, it is not feasible that recognition of Uev1A and cleavage of the linked calicheamicin could kill cancer cells alone. How would a therapy that would use Uev1A-specific Mabs specifically target cancer cells? One possibitity would be to link a Uev1A-specific Mab to calicheamicin and another cancer cell surface-specific molecule. But in that case, would the Uev1A-specific Mab add any killing potential or is the cancer cell surface binding molecule of more therapeutic value? Uev1A-specific Mabs may be of potential value for escalating the explicit cell killing from the inside of a cancer cell if employed with a linked cell-killing agent and cancer cell surface-specific molecule. In this way, the exterior of a cancer cell would be differentiated by the cell surface-specific linked molecule, would be taken up by the cancer cell and once bound to Uev1A, calicheamicin would be released to kill the cells. However, it remains uncertain at this time as to whether the Uev1A-specific Mabs will be useful for cancer therapeutics.

5.9 Significance of these research findings

The development and characteriation of four Uev1A-specific Mabs (LN1, LN2, LN2A and LN2B) and one Uev1A-nonspecific Mab (LN3) will allow research labs to employ molecular and biochemical techniques in order to discover novel findings with respect to Uev1A function in eukaryotic cells. To date, these Uev1A-specific Mabs are the only reagents known to differentiate Uev1A from Mms2 in the world. The overall implications of these Uev1A-specific Mabs are unknown at this time. However, the potential uses for them may be widespread from research and diagnostics in a laboratory to potential anti-cancer pharmaceuticals.

REFERENCES

Albanell, J., J. Codony, A. Rovira, B. Mellado, and P. Gascon. 2003. Mechanism of action of anti-HER2 monoclonal antibodies: scientific update on trastuzumab and 2C4. *Adv Exp Med Biol*. 532:253-68.

Alinari, L., R. Lapalombella, L. Andritsos, R.A. Baiocchi, T.S. Lin, and J.C. Byrd. 2007. Alemtuzumab (Campath-1H) in the treatment of chronic lymphocytic leukemia. *Oncogene*. 26:3644-53.

Ambrus, J.L., Jr., and A.S. Fauci. 1985. Human B lymphoma cell line producing B cell growth factor. *J Clin Invest*. 75:732-9.

Andersen, P.L., H. Zhou, L. Pastushok, T. Moraes, S. McKenna, B. Ziola, M.J. Ellison, V.M. Dixit, and W. Xiao. 2005. Distinct regulation of Ubc13 functions by the two ubiquitin-conjugating enzyme variants Mms2 and Uev1A. *J Cell Biol*. 170:745-55.

Beg, A.A., and D. Baltimore. 1996. An essential role for NF-kappaB in preventing TNF-alpha-induced cell death. *Science*. 274:782-4.

Beg, A.A., W.C. Sha, R.T. Bronson, S. Ghosh, and D. Baltimore. 1995. Embryonic lethality and liver degeneration in mice lacking the RelA component of NF-kappa B. *Nature*. 376:167-70.

Bothos, J., M.K. Summers, M. Venere, D.M. Scolnick, and T.D. Halazonetis. 2003. The Chfr mitotic checkpoint protein functions with Ubc13-Mms2 to form Lys63-linked polyubiquitin chains. *Oncogene*. 22:7101-7.

Bothwell, A.L., M. Paskind, M. Reth, T. Imanishi-Kari, K. Rajewsky, and D. Baltimore. 1981. Heavy chain variable region contribution to the NPb family of antibodies: somatic mutation evident in a gamma 2a variable region. *Cell*. 24:625-37.

Broomfield, S., B.L. Chow, and W. Xiao. 1998. MMS2, encoding a ubiquitin-conjugating-enzyme-like protein, is a member of the yeast error-free postreplication repair pathway. *Proc Natl Acad Sci U S A*. 95:5678-83.

Capra, J.D., A.S. Tung, and A. Nisonoff. 1975. Structural studies on induced antibodies with defined idiotypic specificities. II. The light chains of anti-p-azophenylarsonate antibodies from A/J mice bearing a cross-reactive idiotype. *J Immunol*. 115:414-8.

Carter, P. 2001. Improving the efficacy of antibody-based cancer therapies. *Nat Rev Cancer*. 1:118-29.

Chau, V., J.W. Tobias, A. Bachmair, D. Marriott, D.J. Ecker, D.K. Gonda, and A. Varshavsky. 1989. A multiubiquitin chain is confined to specific lysine in a targeted short-lived protein. *Science*. 243:1576-83.

de StGroth, S.F., and D. Scheidegger. 1980. Production of monoclonal antibodies: strategy and tactics. *J Immunol Methods*. 35:1-21.

Deng, L., C. Wang, E. Spencer, L. Yang, A. Braun, J. You, C. Slaughter, C. Pickart, and Z.J. Chen. 2000. Activation of the IkappaB kinase complex by TRAF6 requires a dimeric ubiquitin-conjugating enzyme complex and a unique polyubiquitin chain. *Cell*. 103:351-61.

Doronina, S.O., B.E. Toki, M.Y. Torgov, B.A. Mendelsohn, C.G. Cerveny, D.F. Chace, R.L. DeBlanc, R.P. Gearing, T.D. Bovee, C.B. Siegall, J.A. Francisco, A.F. Wahl, D.L. Meyer, and P.D. Senter. 2003. Development of potent monoclonal antibody auristatin conjugates for cancer therapy. *Nat Biotechnol*. 21:778-84.

Dreyer, W.J., and J.C. Bennett. 1965. The molecular basis of antibody formation: a paradox. *Proc Natl Acad Sci U S A*. 54:864-9.

Gilmore, T.D. 2006. Introduction to NF-kappaB: players, pathways, perspectives. *Oncogene*. 25:6680-4.

Hager-Braun, C., and K.B. Tomer. 2005. Determination of protein-derived epitopes by mass spectrometry. *Expert Rev Proteomics*. 2:745-56.

Hamblett, K.J., P.D. Senter, D.F. Chace, M.M. Sun, J. Lenox, C.G. Cerveny, K.M. Kissler, S.X. Bernhardt, A.K. Kopcha, R.F. Zabinski, D.L. Meyer, and J.A. Francisco. 2004. Effects of drug loading on the antitumor activity of a monoclonal antibody drug conjugate. *Clin Cancer Res*. 10:7063-70.

Hau, D.D., M.J. Lewis, L.F. Saltibus, L. Pastushok, W. Xiao, and L. Spyracopoulos. 2006. Structure and interactions of the ubiquitin-conjugating enzyme variant human Uev1a: implications for enzymatic synthesis of polyubiquitin chains. *Biochemistry*. 45:9866-77.

Hayden, M.S., and S. Ghosh. 2004. Signaling to NF-kappaB. *Genes Dev*. 18:2195-224.

Herbert, W.J., S. Selwyn, and J.R. Philp. 1965. Field Trials of Adjuvant and Saline Influenza Vaccines. *Br J Prev Soc Med*. 19:97-100.

Hershko, A. 1998. The ubiquitin system. *Annu Rev Biochem*. 67:425-79.

Hershko, A., and A. Ciechanover. 1992. The ubiquitin system for protein degradation. *Annu Rev Biochem*. 61:761-807.

Hochstrasser, M. 1996. Ubiquitin-dependent protein degradation. *Annu Rev Genet.* 30:405-39.

Hoege, C., B. Pfander, G.L. Moldovan, G. Pyrowolakis, and S. Jentsch. 2002. RAD6-dependent DNA repair is linked to modification of PCNA by ubiquitin and SUMO. *Nature*. 419:135-41.

Hofmann, R.M., and C.M. Pickart. 1999. Noncanonical MMS2-encoded ubiquitin-conjugating enzyme functions in assembly of novel polyubiquitin chains for DNA repair. *Cell*. 96:645-53.

Karin, M., and Y. Ben-Neriah. 2000. Phosphorylation meets ubiquitination: the control of NF-[kappa]B activity. *Annu Rev Immunol*. 18:621-63.

Kocks, C., and K. Rajewsky. 1989. Stable expression and somatic hypermutation of antibody V regions in B-cell developmental pathways. *Annu Rev Immunol*. 7:537-59.

Kohler, G., and C. Milstein. 1975. Continuous cultures of fused cells secreting antibody of predefined specificity. *Nature*. 256:495-7.

Kramer, I., and H.P. Lipp. 2007. Bevacizumab, a humanized anti-angiogenic monoclonal antibody for the treatment of colorectal cancer. *J Clin Pharm Ther*. 32:1-14.

Krieger, J.I., S.F. Grammer, H.M. Grey, and R.W. Chesnut. 1985. Antigen presentation by splenic B cells: resting B cells are ineffective, whereas activated B cells are effective accessory cells for T cell responses. *J Immunol*. 135:2937-45.

Kucharczak, J., M.J. Simmons, Y. Fan, and C. Gelinas. 2003. To be, or not to be: NF-kappaB is the answer--role of Rel/NF-kappaB in the regulation of apoptosis. *Oncogene*. 22:8961-82.

Lamothe, B., A. Besse, A.D. Campos, W.K. Webster, H. Wu, and B.G. Darnay. 2007. Site-specific Lys-63-linked tumor necrosis factor receptor-associated factor 6 auto-ubiquitination is a critical determinant of I kappa B kinase activation. *J Biol Chem*. 282:4102-12.

Lin, A., and M. Karin. 2003. NF-kappaB in cancer: a marked target. *Semin Cancer Biol*. 13:107-14.

Littlefield, J.W. 1964. The Selection of Hybrid Mouse Fibroblasts. *Cold Spring Harb Symp Quant Biol*. 29:161-6.

Ma, L., S. Broomfield, C. Lavery, S.L. Lin, W. Xiao, and S. Bacchetti. 1998. Up-regulation of CIR1/CROC1 expression upon cell immortalization and in tumor-derived human cell lines. *Oncogene*. 17:1321-6.

McKenna, S., T. Moraes, L. Pastushok, C. Ptak, W. Xiao, L. Spyracopoulos, and M.J. Ellison. 2003. An NMR-based model of the ubiquitin-bound human ubiquitin conjugation complex Mms2.Ubc13. The structural basis for lysine 63 chain catalysis. *J Biol Chem*. 278:13151-8.

McKenna, S., L. Spyracopoulos, T. Moraes, L. Pastushok, C. Ptak, W. Xiao, and M.J. Ellison. 2001. Noncovalent interaction between ubiquitin and the human DNA repair protein Mms2 is required for Ubc13-mediated polyubiquitination. *J Biol Chem*. 276:40120-6.

Mestas, J., and C.C. Hughes. 2004. Of mice and not men: differences between mouse and human immunology. *J Immunol*. 172:2731-8.

Moraes, T.F., R.A. Edwards, S. McKenna, L. Pastushok, W. Xiao, J.N. Glover, and M.J. Ellison. 2001. Crystal structure of the human ubiquitin conjugating enzyme complex, hMms2-hUbc13. *Nat Struct Biol*. 8:669-73.

Natvig, J.B., and H.G. Kunkel. 1973. Human immunoglobulins: classes, subclasses, genetic variants, and idiotypes. *Adv Immunol*. 16:1-59.

Neuberger, M.S., G.T. Williams, E.B. Mitchell, S.S. Jouhal, J.G. Flanagan, and T.H. Rabbitts. 1985. A hapten-specific chimaeric IgE antibody with human physiological effector function. *Nature*. 314:268-70.

O'Kennedy, R., and P. Roben. 1991. Antibody engineering: an overview. *Essays Biochem*. 26:59-75.

Ollila, J., and M. Vihinen. 2005. B cells. *Int J Biochem Cell Biol*. 37:518-23.

Papa, S., F. Zazzeroni, C.G. Pham, C. Bubici, and G. Franzoso. 2004. Linking JNK signaling to NF-kappaB: a key to survival. *J Cell Sci*. 117:5197-208.

Pastushok, L., T.F. Moraes, M.J. Ellison, and W. Xiao. 2005. A single Mms2 "key" residue insertion into a Ubc13 pocket determines the interface specificity of a human Lys63 ubiquitin conjugation complex. *J Biol Chem*. 280:17891-900.

Perkins, N.D. 2006. Post-translational modifications regulating the activity and function of the nuclear factor kappa B pathway. *Oncogene*. 25:6717-30.

Plosker, G.L., and D.P. Figgitt. 2003. Rituximab: a review of its use in non-Hodgkin's lymphoma and chronic lymphocytic leukaemia. *Drugs*. 63:803-43.

Porter, R.R. 1959. The hydrolysis of rabbit y-globulin and antibodies with crystalline papain. *Biochem J*. 73:119-26.

Prakash, S., P. Sung, and L. Prakash. 1993. DNA repair genes and proteins of Saccharomyces cerevisiae. *Annu Rev Genet*. 27:33-70.

Reinherz, E.L., L. Moretta, M. Roper, J.M. Breard, M.C. Mingari, M.D. Cooper, and S.F. Schlossman. 1980. Human T lymphocyte subpopulations defined by Fc receptors and monoclonal antibodies. A comparison. *J Exp Med*. 151:969-74.

Ricart, A.D., and A.W. Tolcher. 2007. Technology insight: cytotoxic drug immunoconjugates for cancer therapy. *Nat Clin Pract Oncol*. 4:245-55.

Riesen, W. 1980. [Structure and biological properties of immunoglobulins and gamma-globulin preparations. I. Structure and function of immunoglobulins]. *Schweiz Med Wochenschr*. 110:74-9.

Rothofsky, M.L., and S.L. Lin. 1997. CROC-1 encodes a protein which mediates transcriptional activation of the human FOS promoter. *Gene*. 195:141-9.

Sakon, S., X. Xue, M. Takekawa, T. Sasazuki, T. Okazaki, Y. Kojima, J.H. Piao, H. Yagita, K. Okumura, T. Doi, and H. Nakano. 2003. NF-kappaB inhibits TNF-induced accumulation of ROS that mediate prolonged MAPK activation and necrotic cell death. *Embo J*. 22:3898-909.

Sambrook, J., Fritsch, E.F., Maniatis T., Eds. 1989. Molecular Cloning: A Laboratory Manual Second Edition. Cold Spring Harbor Laboratory Press New York.

Sancho, E., M.R. Vila, L. Sanchez-Pulido, J.J. Lozano, R. Paciucci, M. Nadal, M. Fox, C. Harvey, B. Bercovich, N. Loukili, A. Ciechanover, S.L. Lin, F. Sanz, X. Estivill, A. Valencia, and T.M. Thomson. 1998. Role of UEV-1, an inactive variant of the E2 ubiquitin-conjugating enzymes, in in vitro differentiation and cell cycle behavior of HT-29-M6 intestinal mucosecretory cells. *Mol Cell Biol*. 18:576-89.

Schatz, D.G. 2004. V(D)J recombination. *Immunol Rev*. 200:5-11.

Senftleben, U., Y. Cao, G. Xiao, F.R. Greten, G. Krahn, G. Bonizzi, Y. Chen, Y. Hu, A. Fong, S.C. Sun, and M. Karin. 2001. Activation by IKKalpha of a second, evolutionary conserved, NF-kappa B signaling pathway. *Science*. 293:1495-9.

Spiegelberg, H.L. 1974. Biological activities of immunoglobulins of different classes and subclasses. *Adv Immunol*. 19:259-94.

Syed, N.A., P.L. Andersen, R.C. Warrington, and W. Xiao. 2006. Uev1A, a ubiquitin conjugating enzyme variant, inhibits stress-induced apoptosis through NF-kappaB activation. *Apoptosis*. 11:2147-57.

Thorpe, S.J., C. Turner, A. Heath, I. Feavers, I. Vatn, J.B. Natvig, and K.M. Thompson. 2003. Clonal analysis of a human antimouse antibody (HAMA) response. *Scand J Immunol*. 57:85-92.

Tonegawa, S., N. Hozumi, G. Matthyssens, and R. Schuller. 1977. Somatic changes in the content and context of immunoglobulin genes. *Cold Spring Harb Symp Quant Biol*. 41 Pt 2:877-89.

Tyagi, R., R. Lai, and R.G. Duggleby. 2004. A new approach to 'megaprimer' polymerase chain reaction mutagenesis without an intermediate gel purification step. *BMC Biotechnol*. 4:2.

Uhr, J.W., and G. Moller. 1968. Regulatory effect of antibody on the immune response. *Adv Immunol*. 8:81-127.

Van Antwerp, D.J., S.J. Martin, T. Kafri, D.R. Green, and I.M. Verma. 1996. Suppression of TNF-alpha-induced apoptosis by NF-kappaB. *Science*. 274:787-9.

Volk, S., M. Wang, and C.M. Pickart. 2005. Chemical and genetic strategies for manipulating polyubiquitin chain structure. *Methods Enzymol*. 399:3-20.

Wertz, I.E., K.M. O'Rourke, H. Zhou, M. Eby, L. Aravind, S. Seshagiri, P. Wu, C. Wiesmann, R. Baker, D.L. Boone, A. Ma, E.V. Koonin, and V.M. Dixit. 2004. De-ubiquitination and ubiquitin ligase domains of A20 downregulate NF-kappaB signalling. *Nature*. 430:694-9.

Wong, S.F. 2005. Cetuximab: an epidermal growth factor receptor monoclonal antibody for the treatment of colorectal cancer. *Clin Ther*. 27:684-94.

Wu, A.M., and P.D. Senter. 2005. Arming antibodies: prospects and challenges for immunoconjugates. *Nat Biotechnol*. 23:1137-46.

Xiao, L., U.M. Morgan, J. Limor, A. Escalante, M. Arrowood, W. Shulaw, R.C. Thompson, R. Fayer, and A.A. Lal. 1999. Genetic diversity within Cryptosporidium parvum and related Cryptosporidium species. *Appl Environ Microbiol*. 65:3386-91.

Ziola, B., S.L. Gares, B. Lorrain, L. Gee, W.M. Ingledew, and S.Y. Lee. 1999. Epitope mapping of monoclonal antibodies specific for the directly cross-linked mesodiaminopimelic acid peptidoglycan found in the anaerobic beer spoilage bacterium Pectinatus cerevisiiphilus. *Can J Microbiol*. 45:779-85.

APPENDIX A- Solutions, buffers and media

6.1 Chemicals, media and reagents

Agarose gel	0.6% agarose in 1X TAE buffer
Alkaline phosphatase buffer	100 mM Tris, 100 mM NaCl, 5 mM MgCl2, pH 9.5
Alpha calf bovine immunoglobulin depleted serum	Gibco, 200-6200-AJ
Blocking solution	PBST, 5% non-fat milk powder
Bovine albumin	Sigma, #A-7906
5-bromo-4-chloro-3-indolyl phosphate	Bio-Rad, #170-6539
Calf supreme bovine immunoglobulin Serum	Hyclone, #A-2161-L
Cleavage buffer	50 mM Tris-amino, 100 mM NaCl, 1 mM EDTA, pH 8.0
Coomassie blue stain	0.025% Coomassie Brilliant Blue R250, 40% methanol, 7% acetic acid
Copper sulphate	VWR international
Cytoseal mounting medium	Richard Allen Scientific, #8310-16
diaminobenzidine	Envison Plus HRP Kit, Dako #K4007
De-stain solution	40% methanol, 10% acetic acid
EIA assay diluent	1X PBS, 2% Tween 20, 2% bovine albumin, 2 mM merthiolate
Envision Dako Kit	Dako #K4007
Ethanol	VWR international
Ethidium bromide	Sigma, #E8751
Goat-Anti-GST Antibody	GE healthcare, #27-4577-01
Goat-Anti-Mouse IgG, H & L	

Alkaline Phosphatase Conjugated	Calbiochem, #401212
Glutathione elution buffer	10 mM glutathione in 50 mM Tris-HCl, pH 8.0
HAT	Boehringer mannheim
Haematoxlin 1	Richard Allen Scientific, 8310-10
Hydrogen peroxide	VWR international
Immunhistochemistry antibody-dilution buffer	Dako, #S3O22, (0.05 mol/L Tris-HCl, 0.1% Tween, 0.015 mol/L sodium azide).
Luria broth	1% Bacto-tryptone, 0.5% Bacto-yeast extract, 1% NaCl, pH 7.0
Luria agar	US Biological, #L1500
Methanol	VWR international
nitroblue tetrazolium chloride	Bio-Rad, #170-6532
PBST	PBS, 0.05%Tween20
PEG 1500 in 75mM Hepes	Boehringer mannheim
Phosphate buffered saline	140 mM NaCl, 2.7 mM KCl, 10 mM Na_2HPO_4, 1.8 mM KH_2PO_4, pH 7.3
Protein sample buffer	125 mM Tris pH 6.8, 4% SDS, 10% glycerol, 0.006% bromophenol blue, 1.8% β-mercaptoethanol
PVDF membranes	Perkin-Elmer, #NEF1002
Rabbitt-Anti-Goat IgG, H & L Chain alkaline phosphatase conjugated	Calbiochem, #401512
RPMI 1640 S-O media (serum free)	RPMI 1640
RPMI 1640 S-10 media	RPMI 1640, 0.1% mercaptoethanol, 0.01% NaSel, 5% calf supreme bovine immunoglobulin serum and 5% alpha calf bovine immunoglobulin depleted serum (heat inactivated), 0.01% gentamicin

RPMI 1640 HT media	RPMI 1640, 0.1% mercaptoethanol, 0.01% NaSel, 5% calf supreme bovine immunoglobulin serum and 5% alpha calf bovine immunoglobulin depleted serum (heat inactivated), 0.01% gentamicin, and HT
RPMI 1640 HAT media	RPMI 1640, 0.1% mercaptoethanol, 0.01% NaSel, 5% calf supreme bovine immunoglobulin serum and 5% alpha calf bovine immunoglobulin depleted serum (heat inactivated), 0.01% gentamicin, and HAT
SOC	2% Bactro-tryptone, 0.5% Bacto-yeast extract, 0.05% NaCl, 20 mM glucose, 2.5 mM KCl, 10 mM MgCl2, pH 7.0
TAE buffer	24% Tris base, 5.7% glacial acetic acid, 10% EDTA, pH 8.0
Transfer buffer	0.037% SDS, 5.8% Tris-base, 3% (w/v) glycine, 10% methanol
Xylene	VWR international

APPENDIX B –Suppliers

7.1 Antibodies, plasmids, DNA and cell lines

Antibodies used in EIAs:

HRP-conjugated affinity-purified goat anti-mouse H-chain-specific IgG1	Southern Biotechnology Associates Inc.
HRP-conjugated affinity-purified goat anti-mouse H-chain-specific IgG2a	Southern Biotechnology Associates Inc.
HRP-conjugated affinity-purified goat anti-mouse H-chain-specific IgG2b	Southern Biotechnology Associates Inc.
HRP-conjugated affinity-purified goat anti-mouse H-chain-specific IgG3	Southern Biotechnology Associates Inc.
HRP-conjugated affinity-purified goat anti-mouse H-chain-specific IgM	Southern Biotechnology Associates Inc.
HRP-conjugated AffiniPure goat anti-mouse IgG + IgM (H + L chain-specific)	Jackson ImmunoResearch Labs
AffiniPure goat anti-mouse IgG + IgM (H +L chain-specific) minimum cross reaction to human, bovine and horse serum proteins	Jackson ImmunoResearch Labs

Antibodies were supplied by Dr. Barry Ziola

BL21-CodonPlus (DE3)-RIL	Stratagene, #230245
cDNA clones of *MMS2*	Dr. Wei Xiao
cDNA clones of *UEV1A*	Z.J. Chen, university of Texas Southwestern Medical Center, Dallas, TX
cDNA clones of *UEV1B*	S. Lin, Robert Wood Johnson Medical School, Piscataway, NJ
Escherichia coli DH10B	GibcoBRL (now Invitrogen)
pGEX-6P	GE Healthcare, #27-4597-01

PCR primers	IDT, each sequence custom made

7.2 Equipment and supplies

Amicon Ultra centrifugal 54 filter devices	Millipore, #901024
Avanti Beckman centrifuge	Beckman-Coulture, #SJ-1M-1
BCA Protein Assay Kit	Pierce, #23227
Biosafety cabinet	Caltec Scientific, #BM4-2A-49
EIA reader	Bio-Rad, #2550
Envision Dako Kit	Dako, #K4007
Gene Pulser Cuvette	Bio-Rad, #165-2089
GSTrap column (5ml)	GE Healthcare, #17-5131-01
Hydration chambers	Scientific Device Laboratories, #197BL
Immulon 4 flat bottomed plates	Dynatech Labortories Inc, #001-010-3850
Mini-Protean 3 gel apparatus	Bio-Rad, #165-3301
Prescission Protease	GE Healthcare, #27-0843-01
PTC-100 PCR	MJ Research, Inc., Watertown, MA
150 cm^2 tissue culture flask	Corning, #25120
TMB microwell peroxidase substrate	KPL, #50-76-00
UV Transilluminator	Fisher Biotech, #FBTIV-614

7.3 Computer programs

MacReader 2.0 Software	Bio-Rad
PyMOL version 0.96	DeLano Scientific